Accepted Manuscript

Novel glucopyranoside C2-derived 1,2,3-triazoles displaying selective inhibition of *O*-GlcNAcase (OGA)

Michelle O. Igual, Paulo S.G. Nunes, Rafael M. da Costa, Susimaire P. Mantoani, Rita C. Tostes, Ivone Carvalho

PII: S0008-6215(18)30546-9

DOI: https://doi.org/10.1016/j.carres.2018.10.007

Reference: CAR 7617

To appear in: *Carbohydrate Research*

Received Date: 21 September 2018

Revised Date: 19 October 2018

Accepted Date: 22 October 2018

Please cite this article as: M.O. Igual, P.S.G. Nunes, R.M. da Costa, S.P. Mantoani, R.C. Tostes, I. Carvalho, Novel glucopyranoside C2-derived 1,2,3-triazoles displaying selective inhibition of *O*-GlcNAcase (OGA), *Carbohydrate Research* (2018), doi: https://doi.org/10.1016/j.carres.2018.10.007.

Graphical Abstract:

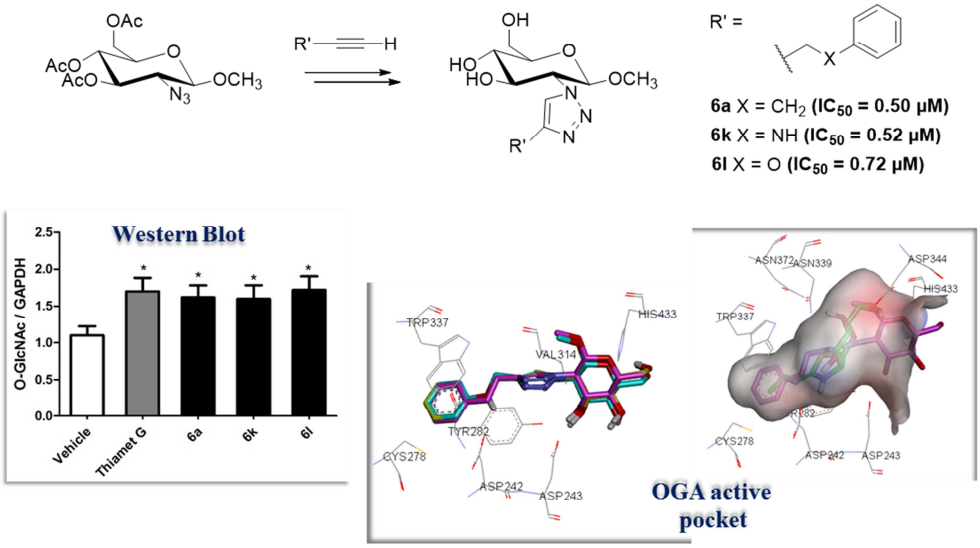

Novel glucopyranoside C2-derived 1,2,3-triazoles displaying selective inhibition of *O*-GlcNAcase (OGA)

Michelle O. Igual,[a] Paulo S. G. Nunes,[a] Rafael M. da Costa,[b] Susimaire P. Mantoani,[a] Rita C. Tostes[b] and Ivone Carvalho[a]*

[a] *School of Pharmaceutical Sciences of Ribeirão Preto, University of São Paulo, Av. do Café s/n, Monte Alegre, 14040-930, Ribeirão Preto, Brazil.*
[b] *Ribeirão Preto Medical School, University of São Paulo, Av. Bandeirantes 3900, Monte Alegre, 14049-900, Ribeirão Preto, Brazil.*

Corresponding author e-mail:* carronal@usp.br

Abstract

O-GlcNAcylation or *O*-GlcNAc modification is a post-translational modification of several proteins responsible for fundamental cellular processes. Dysregulation of the *O*-GlcNAc pathway has been linked to the etiology of several diseases such as neurodegenerative and cardiovascular diseases, type 2 diabetes and cancer. *O*-GlcNAcase (OGA) catalyzes the removal of *O*-GlcNAc from the modified proteins and several carbohydrate-based OGA inhibitors have been synthesized to understand the role of *O*-GlcNAc-modified proteins in physiological and pathological conditions. However, many of the inhibitors lack selectivity for OGA over lysosomal hexosaminidases A and B. Aiming the selectively inhibition of OGA, we propose herein the synthesis of twelve novel glucopyranoside derivatives exploring the bioisosteric replacement of the GlcNAc 2-acetamide group by 1,4-disubstituted 1,2,3-triazole ring, bearing a variety of central chains with different shapes. Compounds were readily prepared through "Copper(I) Catalyzed Azide/Alkyne Cycloaddition" (CuAAC) reaction between a sugar azide and different terminal alkynes. Initial Western Blot analyses and further inhibitory assays proved that compounds **6a** (IC_{50} = 0.50 ± 0.02 µM, OGA), **6k** (IC_{50} = 0.52 ± 0.01 µM, OGA) and **6l** (IC_{50} = 0.72 ± 0.02 µM, OGA) were the most potent and selective compounds of the series. Structure-activity relationship analyses and molecular docking simulations demonstrated that the bridge of two-carbon atoms between the C-4 position of the triazole and the phenyl ring (**6a**), which may be replaced by heteroatoms such as *N* (**6k**) or *O* (**6l**), is fundamental for accommodation and inhibition within OGA catalytic pocket.

Keywords: *O*-GlcNAcase, *O*-GlcNAcylation, selective inhibitors, click chemistry, 1,2,3-triazole

1. Introduction

O-GlcNAcylation or *O*-GlcNAc modification of proteins has been recognized as an important event in the post-translational modification of approximately 4,000 proteins that are responsible for fundamental cellular processes, such as cellular signaling, transcription, protein stability and degradation, among others [1,2]. *O*-GlcNAcylation is directly regulated by two enzymes, a glycosyltransferase named *O*-GlcNAc transferase (OGT), which transfers the sugar *N*-acetylglucosamine (GlcNAc) from uridine 5'-diphosphate *N*-acetylglucosamine (UDP-GlcNAc) substrate to target proteins, and a glycoside hydrolase referred to as *O*-GlcNAcase (OGA), which catalyzes the removal of *O*-GlcNAc from the modified proteins [3].

Dysregulation of the *O*-GlcNAcylation pathway may affect innumerable cell signaling processes [4], contributing to the etiology of several diseases such as neurodegenerative and cardiovascular diseases, type 2 diabetes and cancer [5,2,6]. A range of carbohydrate-based inhibitors of OGA has allowed identification of the role of *O*-GlcNAc-modified proteins in physiological and pathological conditions [7,8]. These inhibitors, which have emerged as novel therapeutic candidates, include PUGNAc, Streptozotocin, NAG-thiazoline, NButGT, Thiamet-G, NAGstatin [8], NAM-thiazolines [9] and, more recently, the thioglycosyl-naphthalimide hybrid molecules CAUS-A and CAUS-B [10] (Figure 1). However, many of them lack selectivity for OGA over lysosomal hexosaminidases, β-*N*-hexosaminidase A (HexA) and β-*N*-hexosaminidase (HexB).

Figure 1.

The cellular activities of OGA and HexA and B can be distinguished owing to the environmental pH and substrate specificity, as observed for OGA activity at neutral pH and GlcNAc substrate, and for HexA and B at acidic (lysosome) pH with affinity for GalNAc units [11]. The role played by the latter on cell metabolism implies that any nonspecific inhibition can give rise to lysosomal ganglioside accumulation that leads to the neurodegenerative Tay-Sachs and Sandhoff diseases [8].

Based on the evidence that the catalytic site of OGA accommodates more flexible and bulky substituents near the 2-acetamide group of the corresponding substrate, compared to HexA and B enzymes, the methyl substituent of the NAG-thiazoline compound (K_I 80 nM) was extended to a propyl group, leading to NButGT (Figure 1) with higher selectivity

(approximately 600-folds for OGA), although with lower potency (K_I 600 nM) [7,12]. Further modifications of the alkyl chain of NButGT through the insertion of an amine group provided Thiamet-G with remarkable potency (K_I 21 nM) and selectivity (37,000-folds) [12].

The achievements on thiazoline-based GlcNAc derivatives encouraged us to pursue an alternative approach to selectively target OGA by exploring the bioisosteric replacement of the GlcNAc 2-acetamide by 1,4-disubstituted 1,2,3-triazole bearing a variety of side chains with different shapes, length and polarity. In fact, triazole-based ring systems have been intensively used in biomedical research in the discovery of new drug candidates and chemical optimization of prototypes [13,14] due to its rigidity, stability and readily preparation using "Copper(I) Catalyzed Azide/Alkyne Cycloaddition" (CuAAC) reaction as a click chemistry strategy [15, 16] to produce easily purified products in good yields.

2. Results and Discussion

2.1. Synthesis of glucopyranoside triazoles library

For the synthesis of glucopyranoside triazole derivatives we followed the 1,3-dipolar cycloaddition (CuAAC) reaction that enables the coupling of the sugar azide with terminal alkynes to afford the acetylated triazole derivatives, which were then deacetylated to give the target compounds.

Based on previously described methods [17,18,19], glucosamine hydrochloride (**1**) was treated with acetyl bromide to give the highly unstable glycosyl bromide, which was immediately used in the next glycosidation step to give the methyl 3,4,6-tri-*O*-acetyl-2-amine-2-deoxy-D-glucopyranoside (**2**), containing the free amine group at the C-2 position (61% yield over two steps, Scheme 1). This approach afforded product **2** as a mixture of β:α anomers in a 10:1 ratio, respectively, that were maintained during its conversion to azide **3** (37%) using diazotransfer reaction in the presence of a freshly prepared triflyl azide solution in pyridine [20,21].

Scheme 1.

For the synthesis of the acetylenic precursors **4g**, **4h**, **4j-l**, different previously reported synthetic approaches were applied. Therefore, treatment of propargylic alcohol with benzyl bromide in dry tetrahydrofuran (THF) [22] afforded alkyne **4g** (66%), while reductive amination between benzaldehyde and propargylamine [23] under the presence of glacial acetic acid (1.0 eq.) [24] gave product **4h** in low yield (24%), though product **4h** was obtained in adequate proportion to proceed with the following cycloaddition reaction. On the

other hand, the amide group of alkyne **4j** (63%) was obtained by the treatment of 4-fluoro-benzoic acid with propargylamine in triethylamine and the coupling reagent *O*-(benzotriazol-1-yl)-*N*,*N*,*N*′,*N*′-tetramethyluronium hexafluorophosphate (HBTU) [25]. For the acetylenes **4k** and **4l**, two similar approaches were used, e.g. potassium carbonate in the presence of 3-bromopropyne treated with aniline [26] to give alkyne **4k** (71%) or with phenol [27] to afford alkyne **4l** (47%). For all the alkyne precursors it was possible to identify the characteristic acetylenes ^{1}H NMR signals, in the range of δ 2.39-2.21 ppm and δ 4.70-3.44 ppm, both presenting propargylic coupling constants (*J* 2.5 – 2.1 Hz).

The CuAAC reactions were carried out with azide precursor **3** and a series of acetylenic precursors (**4a-f** and **4i**, commercially available and **4g**, **4h**, **4j-l** previously synthesized). In general, the acetylated triazole derivatives **5a-l** (Figure 1) were straightforward obtained in moderate to good yields (43-79%) under microwave irradiation at 70 ºC for 10 minutes (min) in dimethylformamide (DMF), in the presence of 0.04 eq. of $CuSO_4$ and 0.1 eq. sodium ascorbate [28]. However, the coupling of acetylenes **4h** and **4k** with azide **3** under these established conditions did not give the corresponding triazoles (**5h**, **5k**), even after two sequential irradiations of 10 min. Therefore, an alternative CuAAC procedure [29] was attempted using the 1,10-phenanthroline monohydrate ligand, in EtOH-H_2O at room temperature in order to increase CuAAC reaction's efficiency, as the 1,10-phenanthroline ligand has been reported to complex with copper(I) allowing its stabilization for the cycloaddition reaction [30,31]. After 18 hours (h), the reaction was completed and products **5h** and **5k** were obtained in 63% and 93% yields, respectively, after chromatographic purification. The ^{1}H NMR spectra of compounds **5a-l** showed characteristic singlet signals in a range of δ 7.55-7.42 ppm for triazole proton, whereas the sugar signals were also observed in all derivatives with typical multiplicity, coupling constant and integrals, notably indicating the downfield shift of the hydrogen at C-2 (δ 4.55-4.28 ppm) compared to their azide precursor **3** (δ 3.51-3.45 ppm).

Finally, deacetylation reaction under standard conditions (catalytic NaOMe/MeOH) [28] gave the glucopyranoside triazoles **6a-l** (Figure 1) in good to excellent yields (59-98%). The absence of ^{1}H NMR singlet signals corresponding to the three acetyl groups was confirmed for all products. Furthermore, it was observed that the hydrogen signals of the free carbohydrate were slightly shifted upfield compared to the acetylated derivatives. The accurate mass of the final compounds **6a-l** was also confirmed by high-resolution mass spectrometry and the data were in accordance with the calculated mass for each compound.

Because of the OGA specificity to β substrates, separation of the anomeric mixture was mandatory. Thus, an expedient separation of the β anomer by reversed phase HPLC was accomplished using polar deacetylated derivatives **6a-l**, though it was laborious and afforded very low quantity of the pure products. To circumvent this issue, we managed to crystallize the precursor azide **3** in EtOH, obtaining the pure β anomer as white needles with 34% yield. Hence, triazole products **6a-l** were promptly obtained as a single β-anomer as depicted in Scheme 1 and then, further submitted to biological assays.

2.2. Cytotoxicity Assay

Prior to testing the potential OGA inhibitory activity of the glucopyranoside triazole library, the 3-(4,5-dimethylthiazol-2-yl)-2,5-diphenyltetrazolium bromide (MTT) assay was performed. The potential toxicity of the glucopyranoside triazole compounds was assessed in cultured vascular smooth muscle cells (VSMC) isolated from aorta of male Wistar rats. The results shown in figure 2 indicate that none of the compounds was cytotoxic against the evaluated cells and, therefore, the compounds were considered suitable for the subsequent studies of inhibitory activity.

Figure 2.

2.3.Inhibitory Activity

The glucopyranoside triazoles **6a-l** were initially obtained as a set of ten compounds **6a-j** and their inhibitory activity over OGA was assessed by Western Blot analysis of *O*-GlcNAc-modified proteins in lysates of cultured VSMCs from aorta of Wistar rats using an antibody anti-β-*O*-linked *N*-acetylglucosamine (Sigma-Aldrich Inc., Germany). As shown in figure 3A, compound **6a**, but not the other compounds from the library **6b-l,** increased *O*-GlcNAc-modified proteins. The Compound **6a** and Thiamet-G produced qualitatively similar increases in *O*-GlcNAc-modified proteins. This preliminary result led us to an interesting structure-activity relationship (SAR) analysis. Among compounds **6a-j**, **6a** is the unique derivative bearing a central chain extension of two-carbon atoms bridging the C-4 position of the triazole core to the phenol ring, suggesting that this length might be critical for accommodation of the inhibitors in the OGA catalytic pocket. Conversely, three-carbon chain displayed by compounds **6f-j** may not adopt the correct orientation within the active site pocket based on the weak ability to enhance protein *O*-GlcNAcylation, as determined in the Western Blot experiments. Further evidence revealed a positive contribution of the aromatic

ring on the activity of compound **6a**, as compound **6e** was not efficient in increasing *O*-GlcNAcylated protein levels. In fact, novel derivatives **6k** and **6l,** containing heteroatoms (*N* or *O*, respectively) that preserve the two carbons bridge extension of **6a** linked to the aromatic ring, exhibited similar activities in the Western Blot assays. These results indicate that compounds **6a**, **6k** and **6l** may create strong interactions at the OGA catalytic pocket, which would enable them to qualitatively augment *O*-GlcNAc levels through OGA inhibition (Figure 3B).

Figure 3.

In order to confirm the ability of the compounds to increase *O*-GlcNAcylation of VSMCs proteins, observed in the Western Blot experiments, OGA enzymatic activity was determined using cell lysates from Wistar rats, as previously described [32]. The enzymatic activity was detected by the fluorescence intensity resulting from the breakdown of 4-methylumbelliferyl *N*-acetyl-β-D-glucosaminide (4-MUNAG) substrate. The percentage of inhibition was calculated by comparing the enzymatic activity in the presence of vehicle or 0.1, 1.0, 10 and 100 µM of the inhibitors. Thiamet-G was used as the reference compound.

Results shown in figure 4 are consistent with the former data, since only compound **6a** decreased OGA activity, by 91% to 93%, at concentrations of 1.0, 10 and 100 µM. Compound **6a** did not display inhibitory activity at lower concentrations, i.e. at 0.1 µM.

Figure 4.

Potential OGA inhibitory activity for compounds **6k** and **6l** was assessed under the same conditions, but using 0.1 and 1.0 µM of the compounds. For comparisons, compound **6a** and Thiamet-G were used. All three compounds were efficient at inhibiting OGA activity at 1.0 µM (Figure 5). Likewise, compounds **6k** and **6l** were equally inactive at the concentration of 0.1 µM. Furthermore, compound **6l,** bearing an additional oxygen atom, showed a lower percentage of inhibition (76%), whereas compound **6k,** bearing an amine group, was very effective, producing inhibitory effects similar to compound **6a** (92%).

Figure 5.

Determination of IC_{50} corroborated the inhibitory activity of compounds **6a**, **6k** and **6l** at micromolar concentrations, with compound **6a** (IC_{50} = 0.50 ± 0.02 µM) and **6k** (IC_{50} = 0.52 ± 0.01 µM) being the most potent followed by compound **6l** (IC_{50} = 0.72 ± 0.02 µM) (Figure 6).

Figure 6.

2.4. Selectivity Assays

The three most active compounds **6a**, **6k** and **6l** were tested against β-*N*-hexosaminidases A and B (HexA and B – GH20 family from prokaryotes) in order to assess their potential selectivity for OGA.

Based on the formerly results obtained in cell lysates, compounds **6a**, **6k** and **6l** were initially evaluated at the concentration of 1.0 µM, whereas Thiamet-G was assayed at 1.0 mM to ensure complete inhibition of the β-*N*-hexosaminidases A and B [33]. Compounds **6a**, **6k** and **6l** did not inhibit HexA or B at 1.0 µM concentration (Figure 7A). These promising results led us to subsequently evaluate the compounds at a higher concentration (1.0 mM). Figure 7B demonstrates that compounds **6a**, **6k** and **6l** inhibited approximately 87% of HexA and B at this concentration.

Figure 7.

IC_{50} determination revealed that compounds **6a** (IC_{50} = 550 ± 0,004 µM), **6k** (IC_{50} = 569 ± 0,009 µM) and **6l** (IC_{50} = 571 ± 0,015 µM) are weak inhibitors of HexA and B (Figure 8), which allowed us to infer a high selective inhibitory effect of these three compounds for OGA over HexA and B.

Figure 8.

2.5.Docking Studies

Molecular docking simulations were performed in order to analyze the binding mode of the most potent inhibitors into the OGA catalytic site. The notable crystal structure of **Bacteroides thetaiotaomicron** OGA (BtOGA) in complex with Thiamet-G (PDB code 2VVN) [33] was chosen to conduct the docking studies, based on its significant sequence identity with the human *O*-GlcNAcase (hOGA) [34]. It is noteworthy that the three-dimensional structure of hOGA was recently determined by Roth and co-workers, revealing addition knowledge of the hOGA active site [35,36].

According to the structural similarity between BtOGA and hOGA, catalytic residues in BtOGA were proposed to be Asp242 and Asp243 [33, 37]. The docking of compounds **6a**, **6k** and **6l** were performed at BtOGA active site in parallel with Thiamet-G [12,33] (Figure 9).

Figure 9.

The docking studies indicated that the two-carbon atoms central chain, bridging the triazole to the phenol ring, from compounds **6a**, **6k** and **6l**, perfectly fit BtOGA catalytic

pocket, being in agreement with the biological assays. Moreover, three compounds display similar conformation within the catalytic site, as can be observed by the superposition of the three structures represented on Figure 9A. Figure 9B shows the conformation of Thiamet-G within BtOGA active site. Figures 9C-E represent compounds **6a**, **6k** and **6l**, respectively, and their interactions with the critical residues in the catalytic pocket.

The phenol ring from compounds **6a**, **6k** and **6l** preserved hydrophobic interactions with Cys278, Tyr282 and Trp337 residues. In addition, the sugar moiety allowed important hydrogen bond interaction with catalytic residue Asp243, and only compound **6k** is capable to perform an addition hydrogen bond interaction with Asp242 (Figure 9D), due to the presence of *N*H group in the central chain bridge, similar to Thiamet-G. Despite the additional interaction of compound **6k** with Asp242, it is observed that it does not significantly influence the inhibitory potency.

Superposition of Thiamet-G and compound **6a** into BtOGA active site, represented on Figure 9F, showed that both compounds occupy the hydrophobic pocket displayed as an extension of the catalytic site of the OGA enzyme. However, the sugar moiety from the triazole derivatives does not occupy the same sugar recognition region of Thiamet-G, as well as of the natural substrate *O*-GlcNAc [38], being displaced outside the catalytic pocket (Figure 9F). On the other hand, the triazole core takes place performing additional interactions that contributes to the activity, and, although the carbohydrate portion is shifted outside the binding region, it is still able to make strong interactions with the key catalytic residues. This observation allows us to the suggestion that the length of the central chain is indeed critical for accommodation of the inhibitors in the OGA catalytic pocket and tightly influence the inhibitory activity of the triazole derivatives over OGA enzyme.

3. Conclusions

We have synthesized twelve novel glucopyranoside triazole derivatives **6a-l**, readily prepared through CuAAC reaction between a sugar azide and different terminal alkynes. MTT assay indicated that none of the compounds was cytotoxic. Screening with Western Blot experiments revealed that compound **6a**, **6k** and **6l** were qualitatively similar to Thiamet-G in augment *O*-GlcNAc-modified proteins levels. Further inhibitory assays showed that compounds **6a**, **6k** and **6l** presented micromolar activity towards OGA with **6a** (IC_{50} = 0.50 ± 0.02 µM) and **6k** (IC_{50} = 0.52 ± 0.01 µM) being the most potent followed by compounds and **6l** (IC_{50} = 0.72 ± 0.02 µM). Moreover, compounds **6a**, **6k** and **6l**

demonstrated highly selectivity for OGA according to the weak inhibition obtained for HexA and B. Additionally, molecular docking studies displayed the interaction mode of the derivatives **6a**, **6k** and **6l** within the OGA catalytic pocket, allowing us to conclude that these compounds occupy all the extension of the catalytic site, being critical for the activity. Furthermore, the sugar moiety from the triazole derivatives occupies a different region in the active site, whilst performing strong interactions, which represents a great factor for the inhibitory activity obtained for the triazole glucopyranoside compounds. These findings provided promising clues for developing more potent OGA inhibitors.

4. Experimental section

4.1. General Information:

All chemicals were acquired as reagent grade (Sigma-Aldrich) and employed without further purification. Solvents were treated according to standard procedures [39]. Reactions were monitored by thin layer chromatography (TLC) on aluminum plates pre-coated with silica gel (60 GF_{254}, Sigma-Aldrich) using the indicated eluents. TLC spots were visualized under ultraviolet (UV) light of 254 nm and/or by staining with ethanol-sulfuric acid (95:5, v/v), ninhydrin or p-anisaldehyde solution followed by heating. Flash chromatography was performed with a column with silica gel 60 (35 – 70 μm) with the indicated eluents. The microwave-assisted reactions were carried out on CEM® Discover System using sealed tubes. ^{1}H and ^{13}C Nuclear Magnetic Resonance spectra were obtained on Bruker Avance DRX 300, DPX 400, DPX 500 spectrometers or Bruker UltraShield 300 FT-NMR spectrometer. Chemical shifts (δ) were reported in parts per million (ppm) downfield from tetramethylsilane (TMS) or relative to the deuterated solvent residual signal (Chloroform-d: δ = 7.26 (^{1}H), 77.16 (^{13}C); Methanol-d_4: δ = 3.31 (^{1}H), 49.00 (^{13}C); Deuterium oxide: 4.79 (^{1}H)). Assignments were made with the aid of COSY, HSQC and HMBC experiments. Optical rotations were measured on a Jasco P-2000 polarimeter at 20 ºC, using sodium lamp and wavelength of 589 nm. High Performance Liquid Chromatograph (HPLC) was performed on a Shimadzu SCL-10AVP, equipped with software CLASS-VP 5.0 and SDP-M10A diode array detector (DAD), using C-18 column (250 x 10 mm, 10 μm, Macherey-Nagel Nucleodur®). High-resolution mass spectra (HRMS) were obtained on a Bruker Daltonics MicrOTOF-Q II ESI-TOF mass spectrometer.

4.2. Synthesis:

4.2.1. Preparation of azide precursor 3

Methyl 3,4,6-tri-*O*-acetyl-2-amino-2-deoxy-D-glucopyranoside (**2**): [17,18,19] Acetyl bromide (3.20 mL; 42.9 mmol) was added to 2-amino-2-deoxy-D-glucose hydrochloride (1.0 g; 4.6 mmol) and the mixture was stirred for 3 days at room temperature. The crude product was dissolved in hot chloroform (distilled from P_2O_5) and filtered while still hot. Brown crystals were formed as the solution cooled off. A small quantity of diethyl ether was added until the solid precipitated from the solution. The product was filtered and washed with diethyl ether. The resulting product was subsequently dissolved in methanol (44 mL) and dry pyridine (0.44 mL) and the mixture was allowed to stir for 1 h at room temperature. The mixture was concentrated by co-evaporation with toluene, diluted in chloroform (60 mL), washed with Na_2CO_3 (aq) (5%, 2 x 100 mL) and water (100 mL), dried over Na_2SO_4, and concentrated. The crude product was recrystallized in chloroform/hexane affording product **2** as a pale yellow solid as a mixture of β/α anomers in the ratio of 10/1, respectively (903.3 mg; 61% yield after two steps). ^{1}H NMR (500 MHz, $CDCl_3$) δ_H: 5.03 – 4.95 (2H, m, H-3, H-4), 4.29 (1H, dd, $J_{5,6a}$ 4.7 Hz, $J_{6a,6b}$ 12.2 Hz, H-6a), 4.16 (1H, d, $J_{1,2}$ 8.0 Hz, H-1), 4.11 (1H, dd, $J_{5,6b}$ 2.2 Hz, $J_{6a,6b}$ 12.2 Hz, H-6b), 3.68 (1H, ddd, $J_{5,4}$ 9.4 Hz, $J_{5,6a}$ 4.7 Hz, $J_{5,6b}$ 2.2 Hz, H-5), 3.55 (3H, s, OCH_3), 2.91 (1H, dd, $J_{1,2}$ 8.0 Hz, $J_{2,3}$ 9.4 Hz, H-2), 2.07, 2.07, 2.01 (9H, 3s, 3 CH_3CO).

Methyl 3,4,6-tri-*O*-acetyl-2-azide-2-deoxy-D-glucopyranoside (**3**): [20,21] A solution of triflyl azide was prepared dissolving sodium azide (170.5 mg; 2.6 mmol) in pyridine (2.9 mL), slowly adding trifluoromethanesulfonic anhydride (0.35 mL; 2.1 mmol) to the mixture at 0 ºC. The mixture was stirred for 2 h at 0 ºC and the precipitated salts were filtered off through celite. The freshly prepared triflyl azide solution was added dropwise at 0 ºC to a solution of compound **2** (578 mg; 1.8 mmol), trimethylamine (0.5 mL; 3.6 mmol) and $CuSO_4$ x 5 H_2O (4.6 mg; 0.018 mmol) in pyridine (2.9 mL). The reaction was carried out for 16 h at room temperature. The mixture was concentrated under reduced pressure followed by purification by flash chromatography [Hexane:EtOAc (1:1)] affording product **3** as a yellow oil as a mixture of β/α (10/1) (233.8 mg; 37% yield). Further crystallization of the β:α mixture with ethanol afforded the β anomer (**3β**) as white needles with 34% yield. ^{1}H NMR (300 MHz, $CDCl_3$) δ_H: 5.05 – 4.96 (2H, m, H-3, H-4), 4.32 – 4.26 (2H, m, H-1, H-6a), 4.12 (1H, dd, $J_{5,6b}$ 2.3 Hz, $J_{6a,6b}$ 12.3 Hz, H-6b), 3.66 (1H, ddd, $J_{5,4}$ 9.6 Hz, $J_{5,6a}$ 4.6 Hz, $J_{5,6b}$ 2.3 Hz, H-5), 3.60 (3H, s, OCH_3), 3.51 – 3.45 (1H, m, H-2), 2.07 (6H, s, 2 CH_3CO), 2.02 (3H, s,

C*H*$_3$CO). ^{13}C NMR (75 MHz, $CDCl_3$) δ_C: 170.8 (*C*OCH$_3$), 170.1 (*C*OCH$_3$), 169.7 (*C*OCH$_3$), 103.0 (C-1), 72.6 (C-5), 71.8 (C-2), 68.4 (C-3), 63.8 (C-4), 62.9 (C-6), 57.6 (O*C*H$_3$), 20.8 (CO*C*H$_3$), 20.8 (CO*C*H$_3$), 20.7 (CO*C*H$_3$). IR (KBr) υ_{max}: 3330, 3231, 2122, 1750, 1392, 1236, 1152, 1048, 607, 496 cm^{-1}.

4.2.2. Synthesis of 1,2,3-triazole-modified glucopyranosides by CuAAC click reaction

General procedure for the synthesis of compounds 5a-g, 5i-j and 5l: [28] Compound **3** containing the azide group (1.0 eq.) was dissolved in DMF (0.3 mL), followed by the addition of sodium ascorbate (0.1 eq.), $CuSO_4$ (10% aqueous solution; 0.04 eq.) and one of the acetylene derivatives (1.0 eq.). The mixture was stirred for 10 min at 70 °C under microwave irradiation (sealed microwave tube) (150 W). The reaction mixture was then concentrated under reduced pressure by co-evaporation with toluene, diluted in water (20 mL) and extracted with EtOAc (3 x 25 mL). The combined organic layers were dried over $MgSO_4$, concentrated under reduced pressure and purified by flash chromatography [Hexane:EtOAc (1:1)] to afford the desired products (**5a-g**, **5i-j** and **5l**).

General procedure for the synthesis of compounds 5h and 5k: [29] A solution of $CuSO_4$ 1.0 M (5 mol%), 1,10-phenanthroline monohydrate (5 mol%), and sodium ascorbate (1.02 eq.) in EtOH–H_2O (2:1 v/v, 6 mL) was allowed to stir for 5 min at room temperature. Subsequently, compound **3** containing the azide group (1.0 eq.) and one of the acetylene derivatives **4h** or **4k** (1.0 eq.) were dissolved in EtOH–H_2O (2:1 v/v, 1 mL) and added to the mixture and the reaction was carried out for 18 h at room temperature. The reaction mixture was then concentrated under reduced pressure and purified by flash chromatography [EtOAc 100%] to afford products (**5h** and **5k**).

Methyl 3,4,6-tri-*O*-acetyl-2-[(4-(phenethyl)-1*H*-1,2,3-triazole-1-yl)]-2-deoxy-β-D-glucopyranoside (**5a**): White solid (108 mg; 73% yield). ^{1}H NMR (300 MHz, $CDCl_3$) δ_H: 7.29 – 7.10 (6H, m, H-triazole, H-Ar.), 5.81 (1H, dd, $J_{2,3}$ 10.7 Hz, $J_{3,4}$ 9.3 Hz, H-3), 5.14 (1H, t, $J_{3,4}$ 9.3 Hz, H-4), 4.91 (1H, d, $J_{1,2}$ 8.2 Hz, H-1), 4.38 (1H, dd, $J_{5,6a}$ 4.4 Hz, $J_{6a,6b}$ 12.3 Hz, H-6a), 4.29 (2H, dd, $J_{1,2}$ 8.2 Hz, $J_{2,3}$ 10.7 Hz, H-2), 4.19 (1H, dd, $J_{5,6b}$ 2.1 Hz, $J_{6a,6b}$ 12.3 Hz, H-6b), 3.91 (1H, ddd, $J_{5,4}$ 9.9 Hz, $J_{5,6a}$ 4.4 Hz, $J_{5,6b}$ 2.1 Hz, H-5), 3.41 (3H, s, OC*H*$_3$), 3.08 – 2.97 (4H, m, C*H*$_2$C*H*$_2$), 2.11, 2.03, 1.80 (9H, 3s, 3 C*H*$_3$CO). ^{13}C NMR (75 MHz, $CDCl_3$) δ_C: 170.8 (*C*OCH$_3$), 169.9 (*C*OCH$_3$), 169.1 (*C*OCH$_3$), 146.8 (C-Ar.), 141.2 (C-triazole), 128.6

(*C*H-Ar.), 128.5 (*C*H-Ar.), 126.1 (*C*H-Ar.), 122.7 (*C*H-triazole), 101.8 (C-1), 72.3 (C-3), 71.9 (C-5), 68.8 (C-4), 63.8 (C-2), 61.9 (C-6), 57.7 (O*C*H_3), 35.4 (*C*H_2), 27.4 (*C*H_2), 20.8 (CO*C*H_3), 20.7 (CO*C*H_3), 20.4 (CO*C*H_3).

Methyl 3,4,6-tri-*O*-acetyl-2-[(4-(benzyl)-1*H*-1,2,3-triazole-1-yl)]-2-deoxy-β-D-glucopyranoside (**5b**): Colorless oil (115.7 mg; 84% yield). ^{1}H NMR (300 MHz, $CDCl_3$) δ_H: 7.33 – 7.20 (5H, m, H-Ar.), 7.15 (1H, s, H-triazole), 5.75 (1H, dd, $J_{2,3}$ 10.6 Hz, $J_{3,4}$ 9.3 Hz, H-3), 5.14 (1H, t, $J_{3,4}$ 9.3 Hz, H-4), 5.00 (1H, d, $J_{1,2}$ 8.2 Hz, H-1), 4.38 (1H, dd, $J_{5,6a}$ 4.6 Hz, $J_{6a,6b}$ 12.4 Hz, H-6a), 4.29 (2H, dd, $J_{1,2}$ 8.2 Hz, $J_{2,3}$ 10.6 Hz, H-2), 4.19 (1H, dd, $J_{5,6b}$ 2.2 Hz, $J_{6a,6b}$ 12.4 Hz, H-6b), 4.13 (1H, d, J_{AB} = 15.9 Hz, CH_a), 4.05 (1H, d, J_{AB} = 15.9 Hz, CH_b), 3.91 (1H, ddd, $J_{5,4}$ 10.1 Hz, $J_{5,6a}$ 4.6 Hz, $J_{5,6b}$ 2.2 Hz, H-5), 3.44 (3H, s, OCH_3), 2.11, 2.03, 1.77 (9H, 3s, 3 CH_3CO). ^{13}C NMR (75 MHz, $CDCl_3$) δ_C: 170.7 (*C*OCH_3), 169.8 (*C*OCH_3), 169.0 (*C*OCH_3), 147.3 (C-triazole), 139.1 (C-Ar.), 128.7 (*C*H-Ar.), 126.6 (*C*H-Ar.), 123.2 (*C*H-triazole), 101.5 (C-1), 72.5 (C-3), 71.9 (C-5), 68.7 (C-4), 63.9 (C-2), 61.9 (C-6), 57.7 (O*C*H_3), 32.1 (*C*H_2), 20.8 (CO*C*H_3), 20.7 (CO*C*H_3), 20.2 (CO*C*H_3).

Methyl 3,4,6-tri-*O*-acetyl-2-[(4-(phenyl)-1*H*-1,2,3-triazole-1-yl)]-2-deoxy-D-glucopyranoside (**5c**): White solid (128.9 mg; 43% yield). ^{1}H NMR (300 MHz, $CDCl_3$) δ_H: 7.84 – 7.81 (2H, m, H-Ar.), 7.75 (1H, s, H-triazole), 7.45 – 7.40 (2H, m, H-Ar.), 7.37 – 7.31 (1H, m, H-Ar.), 5.97 (1H, dd, $J_{2,3}$ 10.4 Hz, $J_{3,4}$ 9.0 Hz, H-3), 5.26 (1H, dd, $J_{3,4}$ 9.0 Hz, $J_{5,4}$ 9.8 Hz, H-4), 5.04 (1H, d, $J_{1,2}$ 7.9 Hz, H-1), 4.55 – 4.47 (2H, m, H-2, H-6a), 4.31 (1H, dd, $J_{5,6b}$ 2.2 Hz, $J_{6a,6b}$ 11.9 Hz, H-6b), 4.06 (1H, ddd, $J_{5,4}$ 9.8 Hz, $J_{5,6a}$ 4.4 Hz, $J_{5,6b}$ 2.2 Hz, H-5), 3.56 (3H, s, OCH_3), 2.28, 2.21, 2.02 (9H, 3s, 3 CH_3CO). ^{13}C NMR (101 MHz, $CDCl_3$) δ_C: 170.7 (*C*OCH_3), 169.9 (*C*OCH_3), 169.2 (*C*OCH_3), 147.4 (C-triazole), 130.3 (C-Ar.), 129.0 (*C*H-Ar.), 128.5 (*C*H-Ar.), 125.8 (*C*H-Ar.), 121.3 (*C*H-triazole), 101.8 (C-1), 72.2 (C-5), 72.1 (C-3), 69.0 (C-4), 64.2 (C-2), 61.9 (C-6), 57.8 (O*C*H_3), 20.8 (CO*C*H_3), 20.7 (CO*C*H_3), 20.4 (CO*C*H_3).

Methyl 3,4,6-tri-*O*-acetyl-2-[(4-(*p*-tolyl)-1*H*-1,2,3-triazole-1-yl)]-2-deoxy-D-glucopyranoside (**5d**): White solid (143.9 mg; 55% yield). ^{1}H NMR (400 MHz, $CDCl_3$) δ_H: 7.74 – 7.72 (3H, m, H-triazole, H-Ar.), 7.24 (2H, d, *J* 7.9 Hz, H-Ar.), 5.92 (1H, dd, $J_{2,3}$ 10.7 Hz, $J_{3,4}$ 9.3 Hz, H-3), 5.19 (1H, t, $J_{3,4}$ 9.3 Hz, H-4), 4.97 (1H, d, $J_{1,2}$ 8.2 Hz, H-1), 4.45 – 4.39 (2H, m, H-2, H-6a), 4.22 (1H, dd, $J_{5,6b}$ 2.3 Hz, $J_{6a,6b}$ 12.3 Hz, H-6b), 3.96 (1H, ddd, $J_{5,4}$ 10.1 Hz, $J_{5,6a}$ 4.5 Hz, $J_{5,6b}$ 2.3 Hz, H-5), 3.44 (3H, s, OCH_3), 2.12, 2.05, 1.85 (9H, 3s, 3 CH_3CO).

^{13}C NMR (101 MHz, $CDCl_3$) δ_C: 170.7 (*C*OCH_3), 169.9 (*C*OCH_3), 169.2 (*C*OCH_3), 147.4 (C-triazole), 138.3 (C-Ar.), 129.6 (*C*H-Ar.), 127.5 (C-Ar.), 125.7 (*C*H-Ar.), 121.0 (*C*H-triazole), 101.8 (C-1), 72.2 (C-5), 72.0 (C-3), 69.0 (C-4), 64.1 (C-2), 61.9 (C-6), 57.8 (O*C*H_3), 21.4 (Ar*C*H_3), 20.8 (CO*C*H_3), 20.7 (CO*C*H_3), 20.4 (CO*C*H_3).

Methyl 3,4,6-tri-*O*-acetyl-2-[(4-(propyl)-1*H*-1,2,3-triazole-1-yl)]-2-deoxy-D-glucopyranoside (**5e**): White solid (124.6 mg; 57% yield). ^{1}H NMR (400 MHz, $CDCl_3$) δ_H: 7.27 (1H, s, H-triazole), 5.81 (1H, dd, $J_{2,3}$ 10.6 Hz, $J_{3,4}$ 9.4 Hz, H-3), 5.16 (1H, t, $J_{3,4}$ 9.4 Hz, H-4), 4.96 (1H, d, $J_{1,2}$ 8.2 Hz, H-1), 4.41 – 4.32 (2H, m, H-2, H-6a), 4.20 (1H, dd, $J_{5,6b}$ 2.2 Hz, $J_{6a,6b}$ 12.3 Hz, H-6b), 3.92 (1H, ddd, $J_{5,4}$ 10.1 Hz, $J_{5,6a}$ 4.5 Hz, $J_{5,6b}$ 2.2 Hz, H-5), 3.43 (3H, s, OC*H*$_3$), 2.69 (2H, t, *J* 7.4 Hz, C*H*$_2$), 2.11, 2.04, 1.84 (9H, 3s, 3 C*H*$_3$CO), 1.69 (2H, m, C*H*$_2$), 0.94 (3H, t, *J* 7.4 Hz, C*H*$_3$). ^{13}C NMR (101 MHz, $CDCl_3$) δ_C: 170.7 (*C*OCH_3), 169.9 (*C*OCH_3), 169.1 (*C*OCH_3), 147.8 (C-triazole), 122.3 (*C*H-triazole), 101.8 (C-1), 72.5 (C-5), 72.0 (C-3), 68.9 (C-4), 63.9 (C-2), 62.0 (C-6), 57.7 (O*C*H_3), 27.6 (*C*H_2), 22.6 (*C*H_2), 20.8 (CO*C*H_3), 20.7 (CO*C*H_3), 20.3 (CO*C*H_3), 13.7 (*C*H_3).

Methyl 3,4,6-tri-*O*-acetyl-2-[(4-(3-phenylpropyl)-1*H*-1,2,3-triazole-1-yl)]-2-deoxy-D-glucopyranoside (**5f**): White solid (157.6 mg; 54% yield). ^{1}H NMR (300 MHz, $CDCl_3$) δ_H: 7.08 – 6.94 (6H, m, H-triazole, H-Ar.), 5.64 (1H, dd, $J_{2,3}$ 10.3 Hz, $J_{3,4}$ 9.0 Hz, H-3), 5.00 (1H, t, $J_{3,4}$ 9.0 Hz, H-4), 4.79 (1H, d, $J_{1,2}$ 8.0 Hz, H-1), 4.28 – 4.18 (2H, m, H-2, H-6a), 4.07 (1H, dd, $J_{5,6b}$ 2.2 Hz, $J_{6a,6b}$ 12.0 Hz, H-6b), 3.80 (1H, ddd, $J_{5,4}$ 9.8 Hz, $J_{5,6a}$ 4.3 Hz, $J_{5,6b}$ 2.2 Hz, H-5), 3.32 (3H, s, OC*H*$_3$), 2.66 (2H, t, *J* 7.4 Hz, C*H*$_2$), 2.58 (2H, t, *J* 7.4 Hz, C*H*$_2$), 2.05, 1.78 (6H, 2s, 2 C*H*$_3$CO), 1.97 – 1.89 (5H, m, C*H*$_3$CO; C*H*$_2$). ^{13}C NMR (75 MHz, $CDCl_3$) δ_C: 170.7 (*C*OCH_3), 169.9 (*C*OCH_3), 169.1 (*C*OCH_3), 147.5 (C-triazole), 141.9 (C-Ar.), 128.6 (*C*H-Ar.), 128.5 (*C*H-Ar.), 126.0 (*C*H-Ar.), 122.4 (*C*H-triazole), 101.7 (C-1), 72.4 (C-3), 72.0 (C-5), 68.8 (C-4), 63.9 (C-2), 61.9 (C-6), 57.7 (O*C*H_3), 35.4 (*C*H_2), 31.0 (*C*H_2), 25.1 (*C*H_2), 20.9 (CO*C*H_3), 20.7 (CO*C*H_3), 20.4 (CO*C*H_3).

Methyl 3,4,6-tri-*O*-acetyl-2-[(4-(benzyloxymethyl)-1*H*-1,2,3-triazole-1-yl)]-2-deoxy-D-glucopyranoside (**5g**): Yellow oil (203 mg; 79% yield). ^{1}H NMR (300 MHz, $CDCl_3$) δ_H: 7.55 (1H, s, H-triazole), 7.36 – 7.29 (5H, m, H-Ar.), 5.84 (1H, t, $J_{3,4}$ 9.6 Hz, H-3), 5.17 (1H, t, $J_{3,4}$ 9.6 Hz, H-4), 4.94 (1H, d, $J_{1,2}$ 8.2 Hz, H-1), 4.67 (2H, s, C*H*$_2$-triazole), 4.58 (2H, s, OBn), 4.38 (2H, dd, $J_{5,6a}$ 4.3 Hz, $J_{6a,6b}$ 12.3 Hz, H-2, H-6a), 4.20 (1H, dd, $J_{5,6b}$ 2.2 Hz, $J_{6a,6b}$ 12.3 Hz, H-6b), 3.92 (1H, ddd, $J_{5,4}$ 10.0 Hz, $J_{5,6a}$ 4.3 Hz, $J_{5,6b}$ 2.2 Hz, H-5), 3.42 (3H, s, OC*H*$_3$), 2.11, 2.03, 1.83 (9H, 3s, 3 C*H*$_3$CO). ^{13}C NMR (101 MHz, $CDCl_3$) δ_C: 170.7 (*C*OCH_3), 169.8

(*C*OCH$_3$), 169.2 (*C*OCH$_3$), 137.8 (C-Ar.), 128.6 (*C*H-Ar.), 128.0 (*C*H-Ar.), 128.0 (*C*H-Ar.), 124.2 (*C*H-triazole), 101.6 (C-1), 72.3 (C-3), 72.6 (OBn), 72.0 (C-5), 68.9 (C-4), 64.2 (C-2), 63.7 (*C*H$_2$-triazole), 61.9 (C-6), 57.7 (O*C*H$_3$), 20.8 (CO*C*H$_3$), 20.7 (CO*C*H$_3$), 20.4 (CO*C*H$_3$).

Methyl 3,4,6-tri-*O*-acetyl-2-[(4-((benzylamino)methyl)-1*H*-1,2,3-triazole-1-yl)]-2-deoxy-β-D-glucopyranoside (**5h**): Yellow oil (214 mg; 63% yield). ^{1}H NMR (400 MHz, CDCl$_3$) δ_H: 7.47 (1H, s, H-triazole), 7.33 – 7.28 (5H, m, H-Ar.), 5.83 (1H, dd, $J_{3,2}$ 10.7 Hz, $J_{3,4}$ 9.3 Hz, H-3), 5.17 (1H, t, $J_{3,4}$ 9.3 Hz, H-4), 4.93 (1H, d, $J_{1,2}$ 8.2 Hz, H-1), 4.41 – 4.33 (2H, m, H-2, H-6a), 4.19 (1H, dd, $J_{5,6b}$ 2.2 Hz, $J_{6a,6b}$ 12.3 Hz, H-6b), 3.94 – 3.89 (3H, m, H-5, C*H*$_2$NH), 3.80 (2H, s, C*H*$_2$-triazole), 3.42 (3H, s, OC*H*$_3$), 2.11, 2.03, 1.84 (9H, 3s, 3 C*H*$_3$CO). ^{13}C NMR (101 MHz, CDCl$_3$) δ_C: 170.7 (*C*OCH$_3$), 169.8 (*C*OCH$_3$), 169.2 (*C*OCH$_3$), 146.4 (C-triazole), 139.8 (C-Ar.), 128.6 (*C*H-Ar.), 128.4 (*C*H-Ar.), 127.2 (*C*H-Ar.), 123.4 (*C*H-triazole), 101.7 (C-1), 72.4 (C-3), 72.1 (C-5), 68.9 (C-4), 64.1 (C-2), 61.9 (C-6), 57.7 (O*C*H$_3$), 53.4 (*C*H$_2$NH), 44.1 (*C*H$_2$-triazole), 20.8 (CO*C*H$_3$), 20.7 (CO*C*H$_3$), 20.4 (CO*C*H$_3$).

Methyl 3,4,6-tri-*O*-acetyl-2-[(4-((benzyl(methyl)amino)methyl)-1*H*-1,2,3-triazole-1-yl)]-2-deoxy-D-glucopyranoside (**5i**): Yellow oil (131.5 mg; 60% yield). ^{1}H NMR (300 MHz, CDCl$_3$) δ_H: 7.51 (1H, s, H-triazole), 7.33 – 7.27 (5H, m, H-Ar.), 5.82 (1H, dd, $J_{2,3}$ 10.6 Hz, $J_{3,4}$ 9.4 Hz, H-3), 5.18 (1H, t, $J_{3,4}$ 9.4 Hz, H-4), 4.98 (1H, d, $J_{1,2}$ 8.2 Hz, H-1), 4.42 – 4.35 (2H, m, H-2, H-6a), 4.20 (1H, dd, $J_{5,6b}$ 2.2 Hz, $J_{6a,6b}$ 12.3 Hz, H-6b), 3.93 (1H, ddd, $J_{5,4}$ 10.1 Hz, $J_{5,6a}$ 4.4 Hz, $J_{5,6b}$ 2.2 Hz, H-5), 3.73 (2H, s, C*H*$_2$-triazole), 3.52 (2H, s, NC*H*$_2$-benzyl), 3.43 (3H, s, OC*H*$_3$), 2.22 (3H, s, NC*H*$_3$), 2.12, 2.04, 1.79 (9H, 3s, 3 C*H*$_3$CO). ^{13}C NMR (75 MHz, CDCl$_3$) δ_C: 170.7 (*C*OCH$_3$), 169.8 (*C*OCH$_3$), 169.1 (*C*OCH$_3$), 129.1 (*C*H-Ar.), 128.4 (*C*H-Ar.), 127.2 (*C*H-Ar.), 124.3 (*C*H-triazole), 101.7 (C-1), 72.4 (C-3), 72.0 (C-5), 68.7 (C-4), 64.0 (C-2), 61.9 (C-6), 61.3 (N*C*H$_2$-benzyl), 57.7 (O*C*H$_3$), 52.0 (*C*H$_2$-triazole), 42.1 (N*C*H$_3$), 20.8 (CO*C*H$_3$), 20.7 (CO*C*H$_3$), 20.3 (CO*C*H$_3$).

Methyl 3,4,6-tri-*O*-acetyl-2-[(4-((*p*-fluorobenzamido)methyl)-1*H*-1,2,3-triazole-1-yl)]-2-deoxy-D-glucopyranoside (**5j**): White solid (121.2 mg; 71% yield). ^{1}H NMR (400 MHz, CDCl$_3$) δ_H: 7.82 – 7.79 (2H, m, H-Ar.), 7.62 (1H, s, H-triazole), 7.12 – 7.08 (2H, m, H-Ar.), 7.01 (1H, t, $J_{CH2,NH}$ 5.6 Hz, N*H*), 5.76 (1H, dd, $J_{2,3}$ 10.6 Hz, $J_{3,4}$ 9.3 Hz, H-3), 5.16 (1H, t, $J_{3,4}$ 9.3 Hz, H-4), 4.99 (1H, d, $J_{1,2}$ 8.2 Hz, H-1), 4.72 (1H, dd, J_{AB} = 15.2 Hz, $J_{H,NH}$ = 5.6 Hz, C*H*$_a$), 4.65 (1H, dd, J_{AB} = 15.2 Hz, $J_{H,NH}$ = 5.6 Hz, C*H*$_b$), 4.40 – 4.33 (2H, m, H-2, H-6a), 4.20 (1H, dd, $J_{5,6b}$ 2.3 Hz, $J_{6a,6b}$ 12.4 Hz, H-6b), 3.91 (1H, ddd, $J_{5,4}$ 10.1 Hz, $J_{5,6a}$ 4.5 Hz, $J_{5,6b}$

2.3 Hz, H-5), 3.43 (3H, s, OC*H*$_3$), 2.11, 2.02, 1.81 (9H, 3s, 3 C*H*$_3$CO). ^{13}C NMR (101 MHz, $CDCl_3$) δ_C: 170.7 (*C*OCH$_3$), 169.7 (*C*OCH$_3$), 169.2 (*C*OCH$_3$), 166.4 (*C*ONH), 144.1 (C-triazole), 130.3 (C-Ar., d, $J_{F,C(para)}$ 3.2 Hz), 129.5 (2*C*H-Ar., d, $J_{F,C(meta)}$ 8.7 Hz), 124.1 (*C*H-triazole), 115.8 (2*C*H-Ar., d, $J_{F,C(ortho)}$ 21.9 Hz), 101.5 (C-1), 72.5 (C-3), 72.1 (C-5), 68.8 (C-4), 64.2 (C-2), 61.9 (C-6), 57.7 (O*C*H$_3$), 35.4 (*C*H$_2$), 20.8 (CO*C*H$_3$), 20.7 (CO*C*H$_3$), 20.3 (CO*C*H$_3$).

Methyl 3,4,6-tri-*O*-acetyl-2-[(4-((phenylamino)methyl)-1*H*-1,2,3-triazole-1-yl)]-2-deoxy-β-D-glucopyranoside (**5k**): Yellow oil (136.3 mg; 93% yield). ^{1}H NMR (300 MHz, $CDCl_3$) δ_H: 7.42 (1H, s, H-triazole), 7.19 – 7.14 (2H, m, H-Ar.), 6.75 – 6.71 (1H, m, H-Ar.), 6.66 – 6.62 (2H, m, H-Ar.), 5.78 (1H, dd, $J_{2,3}$ 10.7 Hz, $J_{3,4}$ 9.3 Hz, H-3), 5.14 (1H, t, $J_{3,4}$ 9.3 Hz, H-4), 4.96 (1H, d, $J_{1,2}$ 8.2 Hz, H-1), 4.46 (2H, s, C*H*$_2$-triazole), 4.41 – 4.32 (2H, m, H-2, H-6a), 4.19 (1H, dd, $J_{5,6b}$ 2.2 Hz, $J_{6a,6b}$ 12.4 Hz, H-6b), 3.91 (1H, ddd, $J_{5,4}$ 10.1 Hz, $J_{5,6a}$ 4.5 Hz, $J_{5,6b}$ 2.2 Hz, H-5), 3.41 (3H, s, OC*H*$_3$), 2.11, 2.03, 1.74 (9H, 3s, 3 C*H*$_3$CO). ^{13}C NMR (75 MHz, $CDCl_3$) δ_C: 170.7 (*C*OCH$_3$), 169.8 (*C*OCH$_3$), 169.2 (*C*OCH$_3$), 147.5 (C-Ar.), 145.9 (C-triazole), 129.4 (*C*H-Ar.), 123.3 (*C*H-triazole), 118.2 (*C*H-Ar.), 113.3 (*C*H-Ar.), 101.6 (C-1), 72.3 (C-3), 72.0 (C-5), 68.7 (C-4), 64.0 (C-2), 61.8 (C-6), 57.7 (O*C*H$_3$), 39.9 (*C*H$_2$-triazole), 20.8 (CO*C*H$_3$), 20.7 (CO*C*H$_3$), 20.2 (CO*C*H$_3$).

Methyl 3,4,6-tri-*O*-acetyl-2-[(4-(phenoxymethyl)-1*H*-1,2,3-triazole-1-yl)]-2-deoxy-β-D-glucopyranoside (**5l**): White solid (104.3 mg; 75% yield). ^{1}H NMR (300 MHz, $CDCl_3$) δ_H: 7.59 (1H, s, H-triazole), 7.32 – 7.26 (2H, m, H-Ar.), 6.99 – 6.95 (3H, m, H-Ar.), 5.82 (1H, dd, $J_{2,3}$ 10.7 Hz, $J_{3,4}$ 9.3 Hz, H-3), 5.23 (2H, s, C*H*$_2$-triazole), 5.16 (1H, t, $J_{3,4}$ 9.3 Hz, H-4), 4.97 (1H, d, $J_{1,2}$ 8.2 Hz, H-1), 4.42 – 4.34 (2H, m, H-2, H-6a), 4.20 (1H, dd, $J_{5,6b}$ 2.2 Hz, $J_{6a,6b}$ 12.4 Hz, H-6b), 3.92 (1H, ddd, $J_{5,4}$ 10.1 Hz, $J_{5,6a}$ 4.5 Hz, $J_{5,6b}$ 2.2 Hz, H-5), 3.43 (3H, s, OC*H*$_3$), 2.11, 2.03, 1.76 (9H, 3s, 3 C*H*$_3$CO). ^{13}C NMR (75 MHz, $CDCl_3$) δ_C: 170.8 (*C*OCH$_3$), 169.9 (*C*OCH$_3$), 169.2 (*C*OCH$_3$), 158.1 (C-Ar.), 144.1 (C-triazole), 129.6 (*C*H-Ar.), 124.4 (*C*H-triazole), 121.4 (*C*H-Ar.), 114.9 (*C*H-Ar.), 101.6 (C-1), 72.3 (C-3), 72.0 (C-5), 68.8 (C-4), 64.3 (C-2), 62.1 (*C*H$_2$-triazole), 62.0 (C-6), 57.8 (O*C*H$_3$), 20.8 (CO*C*H$_3$), 20.7 (CO*C*H$_3$), 20.3 (CO*C*H$_3$).

General procedure for deacetylation reactions: [28] Compounds **5a-l** were dissolved in MeOH and treated with sodium methoxide (1.0 M in MeOH) until pH 9–10 was achieved.

The mixtures were stirred for 1 h at room temperature, neutralized with Dowex 50WX8-200 (H^+), filtered and concentrated under reduced pressure affording products **6a-l**.

Methyl 2-[(4-(phenethyl)-1*H*-1,2,3-triazole-1-yl)]-2-deoxy-β-D-glucopyranoside (**6a**): Colorless oil (55.2 mg; 40% yield). $[\alpha]_D^{22.5}$ -1.9 (*c* 1.29, H_2O). ^{1}H NMR (300 MHz, D_2O) δ_H: 7.51 (1H, s, H-triazole), 7.21 – 7.00 (5H, m, H-Ar.), 4.75 (1H, d, $J_{1,2}$ 8.2 Hz, H-1), 4.12 (1H, dd, $J_{1,2}$ 8.2 Hz, $J_{2,3}$ 10.5 Hz, H-2), 3.97 (1H, t, $J_{3,4}$ 8.5 Hz, H-3), 3.85 (1H, d, $J_{6a,6b}$ 12.3 Hz, H-6b), 3.67 (1H, dd, $J_{5,6a}$ 5.4 Hz, $J_{6a,6b}$ 12.3 Hz, H-6a), 3.54 – 3.49 (1H, m, H-5), 3.43 (1H, t, $J_{3,4}$ 8.5 Hz, H-4), 3.21 (3H, s, OC*H*$_3$), 2.97 – 2.83 (4H, m, C*H*$_2$C*H*$_2$). ^{13}C NMR (75 MHz, D_2O) δ_C: 147.3 (C-triazole), 140.9 (C-Ar.), 128.7 (*C*H-Ar.), 128.4 (*C*H-Ar.), 126.1 (*C*H-Ar.), 123.6 (*C*H-triazole), 101.1 (C-1), 76.0 (C-5), 73.3 (C-3), 69.8 (C-4), 66.0 (C-2), 60.4 (C-6), 57.4 (O*C*H$_3$), 34.4 (*C*H$_2$), 26.0 (*C*H$_2$). HRMS-ESI: calcd for $C_{17}H_{23}N_3NaO_5$ $[M + Na]^+$: 372.1530; found: 372.1532.

Methyl 2-[(4-(benzyl)-1*H*-1,2,3-triazole-1-yl)]-2-deoxy-β-D-glucopyranoside (**6b**): Colorless oil (51.9 mg; 62% yield). $[\alpha]_D^{22.5}$ -1.2 (*c* 0.76, H_2O). ^{1}H NMR (300 MHz, D_2O) δ_H: 7.86 (1H, s, H-triazole), 7.38 – 7.25 (5H, m, H-Ar.), 4.91 (1H, d, $J_{1,2}$ 8.3 Hz, H-1), 4.31 (1H, t, $J_{1,2}$ 8.3 Hz, H-2), 4.12 (1H, t, $J_{3,4}$ 8.6 Hz, H-3), 4.07 (2H, s, C*H*$_2$), 3.96 (1H, dd, $J_{5,6b}$ 1.3 Hz, $J_{6a,6b}$ 12.3 Hz, H-6b), 3.79 (1H, dd, $J_{5,6a}$ 5.4 Hz, $J_{6a,6b}$ 12.3 Hz, H-6a), 3.67 – 3.61 (1H, m, H-5), 3.56 (1H, t, $J_{3,4}$ 8.6 Hz, H-4), 3.34 (3H, s, OC*H*$_3$). ^{13}C NMR (75 MHz, D_2O) δ_C: 147.6 (C-triazole), 138.9 (C-Ar.), 128.8 (*C*H-Ar.), 128.5 (*C*H-Ar.), 126.7 (*C*H-Ar.), 123.7 (*C*H-triazole), 101.0 (C-1), 76.0 (C-5), 73.4 (C-3), 69.7 (C-4), 66.1 (C-2), 60.4 (C-6), 57.2 (O*C*H$_3$), 30.8 (*C*H$_2$). HRMS-ESI: calcd for $C_{16}H_{22}N_3O_5$ $[M + H]^+$: 336.1554; found: 336.1553.

Methyl 2-[(4-(phenyl)-1*H*-1,2,3-triazole-1-yl)]-2-deoxy-β-D-glucopyranoside (**6c**): White solid (73 mg; 98% yield). $[\alpha]_D^{22.5}$ +4.3 (*c* 0.41, H_2O). ^{1}H NMR (300 MHz, D_2O) δ_H: 8.44 (1H, s, H-triazole), 7.84 – 7.82 (2H, m, H-Ar.), 7.55 – 7.42 (3H, m, H-Ar.), 5.03 (1H, d, $J_{1,2}$ 8.2 Hz, H-1), 4.43 (1H, dd, $J_{1,2}$ 8.2 Hz, $J_{2,3}$ 10.2 Hz, H-2), 4.23 (1H, dd, $J_{2,3}$ 10.2 Hz, $J_{3,4}$ 8.8 Hz, H-3), 4.00 (1H, dd, $J_{5,6b}$ 1.9 Hz, $J_{6a,6b}$ 12.2 Hz, H-6b), 3.82 (1H, dd, $J_{5,6a}$ 5.3 Hz, $J_{6a,6b}$ 12.2 Hz, H-6a), 3.70 (1H, ddd, $J_{5,4}$ 10.4 Hz, $J_{5,6a}$ 5.3 Hz, $J_{5,6b}$ 1.9 Hz, H-5), 3.61 (1H, t, $J_{3,4}$ 8.8 Hz, H-4), 3.41 (3H, s, OC*H*$_3$). ^{13}C NMR (101 MHz, D_2O) δ_C: 147.6 (C-triazole), 129.3 (C-Ar.), 129.2 (*C*H-Ar.), 129.0 (*C*H-Ar.), 125.8 (*C*H-Ar.), 122.5 (*C*H-triazole), 101.0 (C-1), 76.2 (C-

5), 73.5 (C-3), 69.9 (C-4), 66.4 (C-2), 60.6 (C-6), 57.3 (O*C*H$_3$). HRMS-ESI: calcd for $C_{15}H_{20}N_3O_5$ $[M + H]^+$: 322.1397; found: 322.1396.

Methyl 2-[(4-(*p*-tolyl)-1*H*-1,2,3-triazole-1-yl)]-2-deoxy-β-D-glucopyranoside (**6d**): White solid (49.9 mg; 67% yield). $[\alpha]_D^{22.5}$ +5.1 (*c* 0.55, CH_3OH). ^{1}H NMR (300 MHz, CD_3OD) δ_H: 8.31 (1H, s, H-triazole), 7.71 (2H, d, *J* 7.9 Hz, H-Ar.), 7.26 (2H, d, *J* 7.9 Hz, H-Ar.), 4.24 (1H, dd, $J_{1,2}$ 8.0 Hz, $J_{2,3}$ 10.5 Hz, H-2), 4.15 (1H, dd, $J_{2,3}$ 10.5 Hz, $J_{3,4}$ 8.0 Hz, H-3), 3.97 (1H, dd, $J_{5,6b}$ 1.9 Hz, $J_{6a,6b}$ 11.9 Hz, H-6b), 3.79 (1H, dd, $J_{5,6a}$ 5.1 Hz, $J_{6a,6b}$ 11.9 Hz, H-6a), 3.56 – 3.46 (2H, m, H-4, H-5), 3.42 (3H, s, OC*H*$_3$), 2.37 (3H, s, ArC*H*$_3$). ^{13}C NMR (75 MHz, CD_3OD) δ_C: 148.3 (C-triazole), 139.3 (C-Ar.), 130.6 (*C*H-Ar.), 128.8 (*C*H-Ar.), 126.6 (*C*H-Ar.), 123.1 (*C*H-triazole), 102.8 (C-1), 78.1 (C-5), 75.6 (C-3), 72.0 (C-4), 68.3 (C-2), 62.5 (C-6), 57.3 (O*C*H$_3$), 21.2 (Ar*C*H$_3$). HRMS-ESI: calcd for $C_{16}H_{22}N_3O_5$ $[M + H]^+$: 336.1554; found: 336.1551.

Methyl 2-[(4-(propyl)-1*H*-1,2,3-triazole-1-yl)]-2-deoxy-β-D-glucopyranoside (**6e**): Colorless oil (65.5 mg; 94% yield). $[\alpha]_D^{22.5}$ -3.5 (*c* 1.16, H_2O). ^{1}H NMR (300 MHz, D_2O) δ_H: 7.85 (1H, s, H-triazole), 4.93 (1H, d, $J_{1,2}$ 8.3 Hz, H-1), 4.30 (1H, dd, $J_{1,2}$ 8.3 Hz, $J_{2,3}$ 10.5 Hz, H-2), 4.12 (1H, dd, $J_{2,3}$ 10.5 Hz, $J_{3,4}$ 8.7 Hz, H-3), 3.96 (1H, dd, $J_{5,6b}$ 1.6 Hz, $J_{6a,6b}$ 12.3 Hz, H-6b), 3.78 (1H, dd, $J_{5,6a}$ 5.4 Hz, $J_{6a,6b}$ 12.3 Hz, H-6a), 3.67 – 3.61 (1H, m, H-5), 3.55 (1H, t, $J_{3,4}$ 8.7 Hz, H-4), 3.36 (3H, s, OC*H*$_3$), 2.66 (2H, t, *J* 7.4 Hz, C*H*$_2$), 1.69 – 1.57 (2H, m, C*H*$_2$), 0.87 (3H, t, *J* 7.4 Hz, C*H*$_3$). ^{13}C NMR (75 MHz, D_2O) δ_C: 148.6 (C-triazole), 123.2 (*C*H-triazole), 101.0 (C-1), 76.0 (C-5), 73.4 (C-3), 69.7 (C-4), 66.0 (C-2), 60.4 (C-6), 57.2 (O*C*H$_3$), 26.3 (*C*H$_2$), 21.9 (*C*H$_2$), 12.6 (*C*H$_3$). HRMS-ESI: calcd for $C_{12}H_{22}N_3O_5$ $[M + H]^+$: 288.1554; found: 288.1554.

Methyl 2-[(4-(3-phenylpropyl)-1*H*-1,2,3-triazole-1-yl)]-2-deoxy-β-D-glucopyranoside (**6f**): Colorless oil (87.8 mg; 96% yield). $[\alpha]_D^{23.8}$ +2.3 (*c* 1.33, CH_3OH). ^{1}H NMR (300 MHz, D_2O) δ_H: 7.82 (1H, s, H-triazole), 7.36 – 7.23 (5H, m, H-Ar.), 4.93 (1H, d, $J_{1,2}$ 8.3 Hz, H-1), 4.30 (1H, dd, $J_{1,2}$ 8.3 Hz, $J_{2,3}$ 10.5 Hz, H-2), 4.13 (1H, dd, $J_{2,3}$ 10.5 Hz, $J_{3,4}$ 8.6 Hz, H-3), 3.97 (1H, dd, $J_{5,6b}$ 1.9 Hz, $J_{6a,6b}$ 12.3 Hz, H-6b), 3.79 (1H, dd, $J_{5,6a}$ 5.5 Hz, $J_{6a,6b}$ 12.3 Hz, H-6a), 3.68 – 3.62 (1H, m, H-5), 3.56 (1H, t, $J_{3,4}$ 8.6 Hz, H-4), 3.37 (3H, s, OC*H*$_3$), 2.70 (2H, t, *J* 7.5 Hz, C*H*$_2$), 2.62 (2H, t, *J* 7.5 Hz, C*H*$_2$), 1.96 (2H, quint, *J* 7.5 Hz, C*H*$_2$). ^{13}C NMR (75 MHz, D_2O) δ_C: 148.2 (C-triazole), 142.3 (C-Ar.), 128.5 (*C*H-Ar.), 125.9 (*C*H-Ar.), 123.4 (*C*H-triazole), 101.1 (C-1), 76.0 (C-5), 73.4 (C-3), 69.8 (C-4), 66.0 (C-2), 60.4 (C-6), 57.2

(O*C*H$_3$), 34.0 (*C*H$_2$), 30.0 (*C*H$_2$), 23.7 (*C*H$_2$). HRMS-ESI: calcd for $C_{18}H_{26}N_3O_5$ $[M + H]^+$: 364.1867; found: 364.1865.

Methyl 2-[(4-(benzyloxymethyl)-1*H*-1,2,3-triazole-1-yl)]-2-deoxy-β-D-glucopyranoside (**6g**): Yellow oil (80 mg; 75% yield). $[\alpha]_D^{22.5}$ -2.7 (*c* 0.91, H_2O). ^{1}H NMR (300 MHz, D_2O) δ_H: 8.09 (1H, s, H-triazole), 7.43 – 7.34 (5H, m, H-Ar.), 4.96 (1H, d, $J_{1,2}$ 8.3 Hz, H-1), 4.71 (2H, s, C*H*$_2$-triazole), 4.61 (2H, s, OBn), 4.36 (1H, dd, $J_{1,2}$ 8.3 Hz, $J_{2,3}$ 10.1 Hz, H-2), 4.17 (1H, t, $J_{3,4}$ 8.8 Hz, H-3), 3.97 (1H, dd, $J_{5,6b}$ 1.2 Hz, $J_{6a,6b}$ 12.4 Hz, H-6b), 3.79 (1H, dd, $J_{5,6a}$ 5.4 Hz, $J_{6a,6b}$ 12.4 Hz, H-6a), 3.69 – 3.63 (1H, m, H-5), 3.57 (1H, t, $J_{3,4}$ 8.8 Hz, H-4), 3.37 (3H, s, OC*H*$_3$). ^{13}C NMR (75 MHz, D_2O) δ_C: 144.0 (C-triazole), 136.8 (C-Ar.), 128.7 (*C*H-Ar.), 128.5 (*C*H-Ar.), 128.3 (*C*H-Ar.), 125.5 (*C*H-triazole), 101.0 (C-1), 76.0 (C-5), 73.3 (C-3), 72.1 (OBn), 69.7 (C-4), 66.1 (C-2), 62.1 (*C*H$_2$-triazole), 60.4 (C-6), 57.2 (O*C*H$_3$). HRMS-ESI: calcd for $C_{17}H_{23}N_3NaO_6$ $[M + Na]^+$: 388.1479; found: 388.1480.

Methyl 2-[(4-((benzylamino)methyl)-1*H*-1,2,3-triazole-1-yl)]-2-deoxy-β-D-glucopyranoside (**6h**): Yellow oil (35 mg; 59% yield). $[\alpha]_D^{22.5}$ -1.9 (*c* 1.07, H_2O). ^{1}H NMR (300 MHz, D_2O) δ_H: 7.96 (1H, s, H-triazole), 7.41 – 7.29 (5H, m, H-Ar.), 4.96 (1H, d, $J_{1,2}$ 8.3 Hz, H-1), 4.34 (1H, dd, $J_{1,2}$ 8.3 Hz, $J_{2,3}$ 10.5 Hz, H-2), 4.15 (1H, dd, $J_{2,3}$ 10.5 Hz, $J_{3,4}$ 8.6 Hz, H-3), 3.96 (1H, dd, $J_{5,6b}$ 2.0 Hz, $J_{6a,6b}$ 12.3 Hz, H-6b), 3.88 (2H, s, C*H*$_2$-triazole), 3.81 – 3.75 (3H, m, H-6a, C*H*$_2$NH), 3.68 – 3.62 (1H, m, H-5), 3.56 (1H, t, $J_{3,4}$ 8.6 Hz, H-4), 3.37 (3H, s, OC*H*$_3$). ^{13}C NMR (75 MHz, D_2O) δ_C: 145.2 (C-triazole), 138.2 (C-Ar.), 128.6 (*C*H-Ar.), 127.5 (*C*H-Ar.), 124.6 (*C*H-triazole), 101.0 (C-1), 76.0 (C-5), 73.3 (C-3), 69.7 (C-4), 66.1 (C-2), 60.4 (C-6), 57.2 (O*C*H$_3$), 51.4 (*C*H$_2$NH), 41.8 (*C*H$_2$-triazole). HRMS-ESI: calcd for $C_{17}H_{25}N_4O_5$ $[M + H]^+$: 365.1819; found: 365.1819.

Methyl 2-[(4-((benzyl(methyl)amino)methyl)-1*H*-1,2,3-triazole-1-yl)]-2-deoxy-β-D-glucopyranoside (**6i**): Yellow oil (66 mg; 98% yield). $[\alpha]_D^{22.5}$ -1.5 (*c* 1.53, H_2O). ^{1}H NMR (500 MHz, D_2O) δ_H: 8.04 (1H, s, H-triazole), 7.44 – 7.34 (5H, m, H-Ar.), 4.99 (1H, d, $J_{1,2}$ 8.4 Hz, H-1), 4.39 (1H, dd, $J_{1,2}$ 8.4 Hz, $J_{2,3}$ 10.2 Hz, H-2), 4.20 (1H, dd, $J_{2,3}$ 10.2 Hz, $J_{3,4}$ 9.3 Hz, H-3), 4.00 (1H, d, $J_{6a,6b}$ 12.4 Hz, H-6b), 3.82 (1H, dd, $J_{5,6a}$ 5.7 Hz, $J_{6a,6b}$ 12.4 Hz, H-6a), 3.78 (2H, s, NC*H*$_2$-triazole), 3.70 – 3.67 (1H, m, H-5), 3.62 – 3.59 (3H, m, H-4; NC*H*$_2$-benzil), 3.41 (3H, s, OC*H*$_3$), 2.22 (3H, s NC*H*$_3$). ^{13}C NMR (126 MHz, D_2O) δ_C: 130.1 (*C*H-Ar.), 128.7 (*C*H-Ar.), 127.9 (*C*H-Ar.), 125.8 (*C*H-triazole), 101.3 (C-1), 76.3 (C-5), 73.5 (C-3), 70.0 (C-

4), 66.3 (C-2), 60.7 (C-6), 60.1 (N*C*H_2-benzil), 57.5 (O*C*H_3), 50.0 (N*C*H_2-triazole), 40.8 (N*C*H_3). HRMS-ESI: calcd for $C_{18}H_{27}N_4O_5$ $[M + H]^+$: 379.1976; found: 379.1975.

Methyl 2-[(4-((*p*-fluorobenzamido)methyl)-1*H*-1,2,3-triazole-1-yl)]-2-deoxy-β-D-glucopyranoside (**6j**): Colorless oil (52.5 mg; 98% yield). $[\alpha]_D^{22.5}$ -2.3 (*c* 0.57, H_2O). ^{1}H NMR (300 MHz, D_2O) δ_H: 8.04 (1H, s, H-triazole), 7.80 – 7.76 (2H, m, H-Ar.), 7.23 – 7.17 (2H, m, H-Ar.), 4.96 (1H, d, $J_{1,2}$ 8.3 Hz, H-1), 4.65 (2H, s, C*H*$_2$), 4.34 (1H, dd, $J_{1,2}$ 8.3 Hz, $J_{2,3}$ 10.0 Hz, H-2), 4.15 (1H, t, $J_{3,4}$ 8.7 Hz, H-3), 3.96 (1H, dd, $J_{5,6b}$ 1.1 Hz, $J_{6a,6b}$ 12.4 Hz, H-6b), 3.78 (1H, dd, $J_{5,6a}$ 5.1 Hz, $J_{6a,6b}$ 12.4 Hz, H-6a), 3.68 – 3.63 (1H, m, H-5), 3.56 (1H, t, $J_{3,4}$ 8.7 Hz, H-4), 3.36 (3H, s, OC*H*$_3$). ^{13}C NMR (75 MHz, D_2O) δ_C: 169.8 (*C*ONH), 164.8 (C-Ar., d, $J_{F,C(ipso)}$ 250.3 Hz), 144.7 (C-triazole), 129.6 (2 *C*H-Ar., d, $J_{F,C(meta)}$ 9.4 Hz), 129.4 (C-Ar., d, $J_{F,C(para)}$ 3.2 Hz), 124.1 (*C*H-triazole), 115.6 (2 *C*H-Ar., d, $J_{F,C(ortho)}$ 22.3 Hz), 100.9 (C-1), 76.0 (C-5), 73.3 (C-3), 69.7 (C-4), 66.1 (C-2), 60.4 (C-6), 57.2 (O*C*H_3), 34.9 (*C*H_2). HRMS-ESI: calcd for $C_{17}H_{21}FN_4NaO_6$ $[M + Na]^+$: 419.1337; found: 419.1338.

Methyl 2-[(4-((phenylamino)methyl)-1*H*-1,2,3-triazole-1-yl)]-2-deoxy-β-D-glucopyranoside (**6k**): Yellow oil (81.4 mg; 81% yield). $[\alpha]_D^{22.5}$ +1.4 (*c* 1.22, H_2O). ^{1}H NMR (300 MHz, D_2O) δ_H: 7.92 (1H, s, H-triazole), 7.25 – 7.20 (2H, m, H-Ar.), 6.85 – 6.80 (3H, m, H-Ar.), 4.84 (1H, d, $J_{1,2}$ 8.3 Hz, H-1), 4.43 (2H, s, C*H*$_2$-triazole), 4.28 (1H, dd, $J_{1,2}$ 8.3 Hz, $J_{2,3}$ 10.5 Hz, H-2), 4.12 (1H, dd, $J_{2,3}$ 10.5 Hz, $J_{3,4}$ 8.4 Hz, H-3), 3.95 (1H, dd, $J_{5,6b}$ 1.9 Hz, $J_{6a,6b}$ 12.4 Hz, H-6b), 3.78 (1H, dd, $J_{5,6a}$ 5.4 Hz, $J_{6a,6b}$ 12.4 Hz, H-6a), 3.64 – 3.59 (1H, m, H-5), 3.54 (1H, t, $J_{3,4}$ 8.4 Hz, H-4), 3.25 (3H, s, OC*H*$_3$). ^{13}C NMR (75 MHz, D_2O) δ_C: 146.9 (C-triazole), 146.0 (C-Ar.), 129.4 (*C*H-Ar.), 124.0 (*C*H-triazole), 119.4 (*C*H-Ar.), 115.1 (*C*H-Ar.), 101.0 (C-1), 76.0 (C-5), 73.2 (C-3), 69.7 (C-4), 66.1 (C-2), 60.4 (C-6), 57.3 (O*C*H_3), 38.8 (*C*H_2-triazole). HRMS-ESI: calcd for $C_{16}H_{23}N_4O_5$ $[M + H]^+$: 351.1663; found: 351.1663.

Methyl 2-[(4-(phenoxymethyl)-1*H*-1,2,3-triazole-1-yl)]-2-deoxy-β-D-glucopyranoside (**6l**): White solid (86.3 mg; 98% yield). $[\alpha]_D^{22.5}$ -0.13 (*c* 0.85, H_2O). ^{1}H NMR (300 MHz, D_2O) δ_H: 8.12 (1H, s, H-triazole), 7.36 – 7.31 (2H, m, H-Ar.), 7.06 – 7.01 (3H, m, H-Ar.), 5.23 (2H, s, C*H*$_2$-triazole), 4.89 (1H, d, $J_{1,2}$ 8.3 Hz, H-1), 4.33 (1H, dd, $J_{1,2}$ 8.3 Hz, $J_{2,3}$ 10.6 Hz, H-2), 4.15 (1H, dd, $J_{2,3}$ 10.6 Hz, $J_{3,4}$ 8.5 Hz, H-3), 3.96 (1H, dd, $J_{5,6b}$ 2.0 Hz, $J_{6a,6b}$ 12.4 Hz, H-6b), 3.78 (1H, dd, $J_{5,6a}$ 5.4 Hz, $J_{6a,6b}$ 12.4 Hz, H-6a), 3.65 – 3.60 (1H, m, H-5), 3.55 (1H, t, $J_{3,4}$ 8.5 Hz, H-4), 3.29 (3H, s, OC*H*$_3$). ^{13}C NMR (75 MHz, D_2O) δ_C: 168.2 (C-triazole),

157.0 (C-Ar.), 143.2 (*C*H-triazole), 129.8 (*C*H-Ar.), 122.0 (*C*H-Ar.), 115.5 (*C*H-Ar.), 101.0 (C-1), 76.1 (C-5), 73.3 (C-3), 69.9 (C-4), 66.9 (C-2), 61.1 (CH_2-triazole), 60.5 (C-6), 57.3 (OCH_3). HRMS-ESI: calcd for $C_{16}H_{21}N_3NaO_6$ $[M + Na]^+$: 374.1323; found: 374.1320.

4.3. Biological Assays

4.3.1. Cytotoxicity assay

To determine potential cytotoxic effects of the compounds, the colorimetric assay with 4,5-dimethylthiazol-2-yl)-2,5-diphenyltetrazolium bromide (MTT) was performed [40]. Cultured vascular smooth muscle cells (VSMCs) isolated from aorta of Wistar rats were seeded (100 µl/well) at seeding densities of $1x10^6$ cells/ml into 96-well plates and allowed to adhere for 24 h. VSMCs were incubated with 0.10, 0.25, 0.50, 0.75, 1.0, 10.0 µM of compounds **6a-l** for 6 h in a CO_2 (5%) chamber, at 37 ºC. Following the incubation period, 20 µL of MTT (5 mg/mL) were added to the wells and the plates were incubated at 37 ºC for 4 h. Then, 50 µL isopropanol/HCl were added to the wells and the plates were kept at room temperature for 1 h. The absorbance at 570 nm of the plates was read with the Epoch Microplate Spectrophotometer (BioTek®, Winooski, VT, USA). Absorbance values were blanked against dimethyl sulfoxide (DMSO) and the absorbance of cells exposed to medium only (i.e. no compounds or vehicle added) was taken as 100 % cell viability (i.e. the control).

4.3.2. Western Blot analysis

Western Blot analysis was assessed in lysates of cultured VSMCs from aorta from Wistar rats using antibodies anti-β-*O*-linked *N*-acetylglucosamine, anti-OGA and anti-GAPDH (Sigma-Aldrich Inc., Germany), according to the previously reported method [32].

4.3.3. Enzymatic Activity Assays

O-GlcNAcase OGA) and β-*N*-Acetylhexosaminidase A and B activity were performed as previously described [32]. Proteins were extracted (3 µg), quantified using the Bradford method [41] and eluted in citrate buffer following the procedure reported [32]. IC_{50} measurements of OGA activity against the compounds **6a-l** were performed using the fluorogenic 4-methylumbelliferyl *N*-acetyl-β-D-glucosaminide (4-MUNAG, 300 µg/ml, Sigma-Aldrich Inc., Germany) substrate. After elution, the OGA substrate 4-MUNAG,

compounds **6a-l** or the OGA inhibitor Thiamet-G (positive control), at concentrations of 0.10, 0.25, 0.50, 0.75, 1.0, 10.0 µM were added. Proteins were kept in a chamber at 37 °C for 30 min and the reaction was stopped by addition of glycine buffer (0.1 M, pH 12). The fluorescence of the released 4-MU was quantified after excitation of 362 nm and emission of 448 nm in a FlexStation 3 Multi-Mode Microplate Reader (Molecular Devices®, San Jose, CA, USA). Percent of inhibition was calculated comparing the enzyme activity in the absence of the inhibitors with the activity in the presence of the inhibitors. Assays were performed in triplicate under identical conditions.

β-*N*-Acetylhexosaminidase A and B from prokaryote (EC 3.2.1.52, Megazyme, Ireland, UK) assays toward compounds **6a**, **6k** and **6l** were measured in duplicate under the same conditions as described above.

4.4.Molecular Docking

Ligands were docked *in silico* into the proposed active site of BtOGA (PDB code 2VVN) [33]. All docking runs were performed with the GOLD 5.2 software [42,43]. For the calculations, the orientation of highest score (top-ranked) was selected for each of compounds here investigated. Top-ranked orientations were selected by GOLD via an empirical energy function (the ChemPLP) [44]. Based on this function, the software classifies the orientations of the molecules by a decreasing ordering of affinity (the fitness) with the binding site of the *O*-GlcNAcase. The simulations were performed inside a sphere of 10 Å radius in a point centered among Asp242 and Asp243 catalytic residues and Cys278, Tyr282, TRp337, Asn339 and Asp334 residues, with 100 orientations (docking runs) for each molecule.

5. Acknowledgments

This research was supported by grants from São Paulo Research Foundation (FAPESP Proc. 2016/04003-2), Coordenação de Aperfeiçoamento de Pessoal de Nível Superior (CAPES) and Conselho Nacional de Desenvolvimento Científico e Tecnológico (CNPq).

6. References

[1] J. Ma, G.W. Hart, O-GlcNAc profiling: from proteins to proteomes, Clin. Proteomics. 11 (2014) 1–16. doi:10.1186/1559-0275-11-8.

[2] M.R. Bond, J.A. Hanover, O-GlcNAc cycling: a link between metabolism and chronic disease, Annu. Rev. Nutr. 33 (2013) 205–229. doi: 10.1146/annurev-nutr-071812-161240.

[3] E.J. Kim, Chemical arsenal for the study of O-GlcNAc, Molecules. 16 (2011) 1987–2022. doi: 10.3390/molecules16031987.

[4] Q. Zeidan, G.W. Hart, The intersections between O-GlcNAcylation and phosphorylation: implications for multiple signaling pathways, J. Cell Sci. 123 (2010) 13–22. doi: 10.1242/jcs.053678.

[5] G.W. Hart, M.P. Housley, C. Slawson, Cycling of O-linked β-N-acetylglucosamine on nucleocytoplasmic proteins, Nature. 446 (2007) 1017–1022. doi: 10.1038/nature05815.

[6] M.R. Bond, J.A. Hanover, A little sugar goes a long way: the cell biology of O-GlcNAc, J. Cell Bio. 208 (2015) 869–880. doi: 10.1083/jcb.201501101.

[7] T. Li, L. Guo, Y. Zhang, J. Wang, Z. Li, L. Lin, Z. Zhang, L. Li, J. Lin, W. Zhao, J. Li, P.G. Wang, Design and synthesis of O-GlcNAcase inhibitors via 'click chemistry' and biological evaluations, Carbohydr. Res. 346 (2011) 1083–1092. doi: 10.1016/j.carres.2011.03.026.

[8] M.S. Macauley, D.J. Vocadlo, Increasing O-GlcNAc levels: an overview of small-molecule inhibitors of O-GlcNAcase, Biochim. Biophys. Acta. 1800 (2010) 107–121. doi: 10.1016/j.bbagen.2009.07.028.

[9] H. Kong, W. Chen, T. Liu, H. Lu, Q. Yang, Y. Dong, X. Liang, S. Jin, J. Zhang, Synthesis of NAM-thiazoline derivatives as novel O-GlcNAcase inhibitors, Carbohydr. Res. 429 (2016) 54–61. doi: 10.1016/j.carres.2016.04.008.

[10] W. Chen, S. Shen, L. Dong, J. Zhang, Q. Yang, Selective inhibition of β-N-acetylhexosaminidases by thioglycosyl–naphthalimide hybrid molecules, Bioorg. Med. Chem. 26 (2018) 394–400. doi: 10.1016/j.bmc.2017.11.042.

[11] Y. Gao, L. Wells, F.I. Comer, G.J. Parker, G.W. Hart, Dynamic O-glycosylation of nuclear and cytosolic proteins: cloning and characterization of a neutral, cytosolic β-N-acetylglucosaminidase from human brain, J. Biol. Chem. 276 (2001) 9838–9845. doi: 10.1074/jbc.M010420200.

[12] M.S. Macauley, G.E. Whitworth, A.W. Debowski, D. Chin, D.J. Vocadlo, O-GlcNAcase uses substrate-assisted catalysis: Kinect analysis and development of highly selective mechanism-inspired inhibitors, J. Biol. Chem. 280 (2005) 25313–25322. doi: 10.1074/jbc.M413819200.

[13] H.C. Kolb, K.B. Sharpless, The growing impact of click chemistry on drug discovery, Drug Discov. Today. 8 (2003), 1128–1137. https://doi.org/10.1016/S1359-6446(03)02933-7.

[14] L.V.R. Reddy, P.V. Reddy, N.N. Mishra, P.K. Shukla, G. Yadav, R. Srivastava, A.K. Shaw, Synthesis and biological evaluation of glycal-derived novel tetrahydrofuran 1,2,3-triazoles by 'click' chemistry, Carbohydr. Res. 345 (2010) 1515–1521. doi: 10.1016/j.carres.2010.03.031.

[15] C.W. Tornoe, C. Christensen, M. Meldal, Peptidotriazoles on solid phase: [1,2,3]-triazoles by regiospecific copper(I)-catalyzed 1,3-dipolar cycloadditions of terminal alkynes to azides, J. Org. Chem. 67 (2002) 3057−3064. doi: 10.1021/jo011148j.

[16] V.V. Rostovtsev, L.G. Green, V.V. Fokin, K.B. Sharpless, A stepwise huisgen cycloaddition process: copper(I)-catalyzed regioselective "ligation" of azides and terminal alkynes, Angew. Chem., Int. Ed. Engl. 41 (2002) 2596−2599. doi: 10.1002/1521-3773(20020715)41:14<2596::AID-ANIE2596>3.0.CO;2-4.

[17] J.C. Irvine, D. McNicool, A. Hynd, New Derivatives of d-Glucosamine, J. Chem. Soc., Trans. 99 (1911) 250–261. doi: 10.1039/CT9119900250.

[18] T. Yamasaki, Y. Kubota, T. Tsuchiya, S. Umezawa, Syntheses of 2-Amino-2,3-dideoxy-L- and -D-Ribohexose by Utilizing an O→N Acetyl Migration, Bull. Chem. Soc. Jpn. 49 (1976) 3190–3192. https://doi.org/10.1246/bcsj.49.3190.

[19] J.F. Billing, U.J. Nilsson, Cyclic peptides containing a δ-sugar amino acid – synthesis and evaluation as artificial receptors, Tetrahedron. 61 (2004) 863–874. https://doi.org/10.1016/j.tet.2004.11.024.

[20] K. Günther, C. Schips, T. Ziegler, Preparation of some glycosyl amino acid building blocks via click reaction and construction of a glycotetrapeptide library using spot synthesis, J. Carbohydr. Chem. 27 (2008) 446–463. https://doi.org/10.1080/07328300802419873.

[21] R.-B. Yan, F. Yang, Y. Wu, L.-H. Zhang, X.-S. Ye, An efficient and improved procedure for preparation of triflyl azide and application in catalytic diazotransfer reaction, Tetrahedron Lett. 46 (2005) 8993–8995. doi: 10.1016/j.tetlet.2005.10.103.

[22] D. Farran, A.M.Z. Slawin, P. Kirsch, D. O'hagan, Diastereoselective Synthesis of 2,3,4,5,6-Pentafluoroheptanes, J. Org. Chem. 74 (2009) 7168–7171. doi: 10.1021/jo901360e.

[23] J.M. Krysiak, J. Kreuzer, P. Macheroux, A. Hermetter, S.A. Sieber, R. Breinbauer, Activity-Based Probes for Studying the Activity of Flavin-Dependent Oxidases and for the Protein Target Profiling of Monoamine Oxidase Inhibitors, Angew. Chem. Int. Ed. Engl. 51 (2012) 7035–7040. doi: 10.1002/anie.201201955.

[24] A.F. Abdel-Magid, K.G. Carson, B.D. Harris, C.A. Maryanoff, R.D. Shah, Reductive Amination of aldehydes and ketones with sodium triacetoxyborohydride. Studies on direct and indirect reductive amination procedures, J. Org. Chem. 61 (1996) 3849–3862. doi: 10.1021/jo960057x.

[25] A. Chibba, J. Poloczek, D.J. Little, P.L. Howell, M. Nitz, Synthesis and evaluation of inhibitors of E. coli PgaB, a polysaccharide de-N-acetylase involved in biofilm formation, Org. Biomol. Chem. 10 (2012) 7103–7107. doi: 10.1039/C2OB26105G.

[26] K.C. Majumdar, S. Ganai, An expedient approach to substituted triazolo[1,5-a][1,4]benzodiazepines via Cu-catalyzed tandem Ullmann C–N coupling/azide-alkyne cycloaddition, Tetrahedron Lett. 54 (2013) 6192–6195. https://doi.org/10.1016/j.tetlet.2013.08.125.

[27] W. Zhang, Z. Li, M. Zhou, F. Wu, X. Hou, H. Luo, H. Liu, X. Han, G. Yan, Z. Ding, R. Li, Synthesis and biological evaluation of 4-(1,2,3-triazol-1-yl)coumarin derivatives as potential antitumor agents, Bioorg. Med. Chem. Lett. 24 (2014) 799–807. doi: 10.1016/j.bmcl.2013.12.095.

[28] I. Carvalho, P. Andrade, V.L. Campo, P.M.M. Guedes, R. Sesti-Costa, J.S. Silva, S. Schenkman, S. Dedola, L. Hill, M. Rejzek, S.A. Nepogodiev, R.A. Field, 'Click chemistry' synthesis of a library of 1,2,3-triazole-substituted galactose derivatives and their evaluation against Trypanosoma cruzi and its cell surfacetrans-sialidase, Bioorg. Med. Chem. 18 (2010) 2412–2427. doi: 10.1016/j.bmc.2010.02.053.

[29] D.Y. Cruz-Gonzalez, R. González-Olvera, G.E. Negrón-Silva, L. Lomas-Romero, A. Gutiérrez-Carrillo, M.E. Palomar-Pardavé, M.A. Romero-Romo, R. Santillan, J. Uruchurtu, One-Pot Three-Component Synthesis of New Mono- and Bis-1,2,3-triazole Derivatives of 2-Benzimidazolethiol with a Promising Inhibitory Activity against Acidic Corrosion of Steel, Synthesis. 46 (2014) 1217–1223. doi: 10.1055/s-0033-1340863.

[30] S. Díez-González, Well-defined copper(I) complexes for click azide–alkyne cycloaddition reactions: one click beyond, Catal. Sci. Technol. 1 (2011) 166–178. doi: 10.1039/C0CY00064G.

[31] B.F. Straub, μ-Acetylide and μ-alkenylidene ligands in ''click'' triazole syntheses, Chem. Commun. 0 (2007) 3868–3870. doi: 10.1039/B706926J.

[32] R.M. da Costa, J.F.d. Silva, J.V. Alves, T.B. Dias, D.M. Rassi, L.V. Garcia, N.d.S. Lobato, R.C. Tostes, Increased *O*-GlcNAcylation of Endothelial Nitric Oxide Synthase Compromises the Anti-contractile Properties of Perivascular Adipose Tissue in Metabolic Syndrome, Front. Physiol. 9 (2018) 1–16. doi: 10.3389/fphys.2018.00341.

[33] S. Yuzwa, M.S. Macauley, J.E. Heinonen, X. Shan, R.J. Dennis, Y. He, G.E. Whitworth, K.A. Stubbs, E.J. McEachern, G.J. Davies, D.J. Vocadlo, A potent mechanism-inspired O-GlcNAcase inhibitor that blocks phosphorylation of tau in vivo, Nat. Chem. Biol. 4 (2008) 483–490. doi: 10.1038/nchembio.96.

[34] R.J. Dennis, E.J. Taylor, M.S. Macauley, K.A. Stubbs, J.P. Turkenburg, S.J. Hart, G.N. Black, D.J. Vocadlo, G.J. Davies, Structure and mechanism of a bacterial β-glucosaminidase having O-GlcNAcase activity, Nat. Struct. Mol. Biol. 13 (2006) 365–371. doi: 10.1038/nsmb1079.

[35] C. Roth, S. Chan, W.A. Offen, G.R. Hemsworth, L.I. Willems, D.T. King, V. Varghese, R. Britton, D.J. Vocadlo, G.J. Davies, Structural and functional insight into human O-GlcNAcase, Nat. Chem. Biol. 13 (2017) 610–612. doi: 10.1038/nchembio.2358.

[36] N.L. Elsen, S.B. Patel, R.E. Ford, D.L. Hall, F. Hess, H. Kandula, M. Kornienko, J. Reid, H. Selnick, J. M. Shipman, S. Sharma, K.J. Lumb, S.M. Soisson, D.J. Klein, Insights

into activity and inhibition from the crystal structure of human O-GlcNAcase, Nat. Chem. Biol. 13 (2017) 613–615. doi: 10.1038/nchembio.2357.

[37] N.A.N. de Alencar, P.R.M. Sousa, J.R.A. Silva, J. Lameira, C.N. Alves, S. Martí, V. Moliner, Computational Analysis of Human OGA Structure in Complex with PUGNAc and NAG-Thiazoline Derivatives, J. Chem. Inf. Model. 52 (2012) 2775–2783. doi: 10.1021/ci2006005.

[38] M. Schimpl, V.S. Borodkin, L.J. Gray, D.M.F. van Aalten, Synergy of Peptide and Sugar in *O*-GlcNAcase Substrate Recognition, Chem. Biol. 19 (2012) 173–178. doi: 10.1016/j.chembiol.2012.01.011.

[39] W.L.F. Armarego, C.L.L. Chai, Purification of Laboratory Chemicals, sixth ed., Butterworth-Heinemann, 2009.

[40] T. Mosmann, Rapid colorimetric assay for cellular growth and survival: application to proliferation and cytotoxicity assays, J. lmmunol. Methods. 65 (1983) 55–63. https://doi.org/10.1016/0022-1759(83)90303-4.

[41] M.M. Bradford, A rapid and sensitive method for the quantitation of microgram quantities of protein utilizing the principle of protein-dye binding, Anal. Biochem. 72 (1976) 248–254. https://doi.org/10.1016/0003-2697(76)90527-3.

[42] G. Jones, P. Willett, R.C. Glen, A.R. Leach, R. Taylor, Development And Validation Of A Genetic Algorithm For Flexible Docking, J. Mol. Biol. 267 (1997) 727–748. https://doi.org/10.1006/jmbi.1996.0897.

[43] M.L. Verdonk, J.C. Cole, M.J. Hartshorn, C.W. Murray, R.D. Taylor, Improved protein–ligand docking using GOLD. Proteins. 52 (2003) 609–623. doi: 10.1002/prot.10465.

[44] J.W. Liebeschuetz, J.C. Cole, O. Korb, Pose prediction and virtual screening performance of GOLD scoring functions in a standardized test, J. Comput. Aided. Mol. Des. 26 (2012) 737–748. doi: 10.1007/s10822-012-9551-4.

Figures:

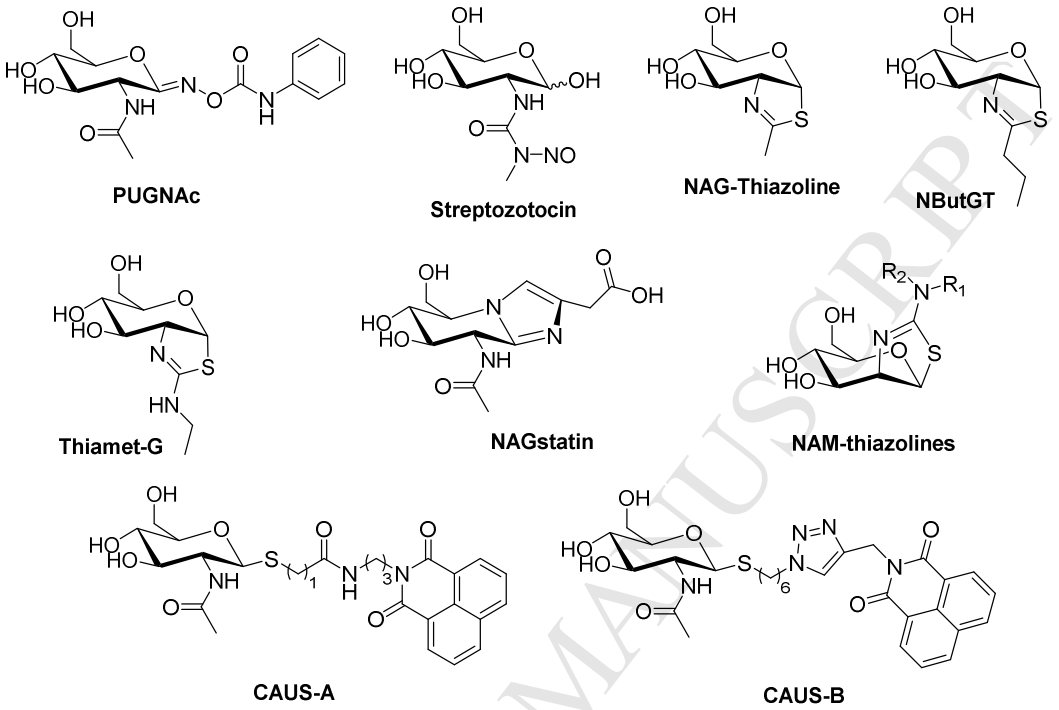

Figure 1. *O*-GlcNAcase (OGA) inhibitors previously reported.

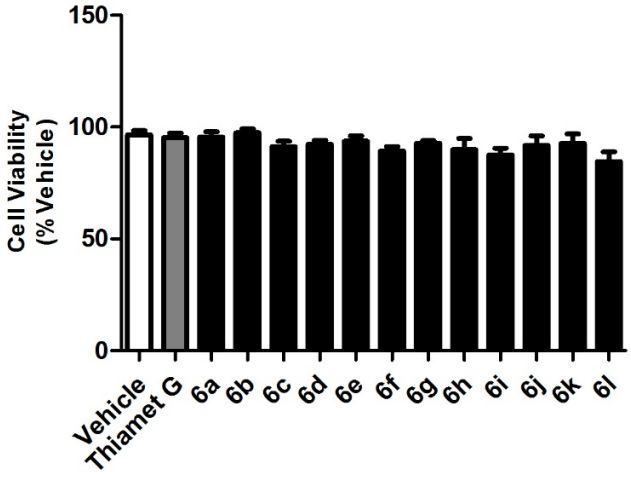

Figure 2. Cell viability assay. Cultured vascular smooth muscle cells were incubated for 6 h with 1.0 µM of the glucopyranoside triazole compounds **6a-l.** The potential cytotoxicity of the compounds was determined with the MTT assay. Results are expressed as mean ± SEM for n=5 in each experimental group. One-way ANOVA.

(B)

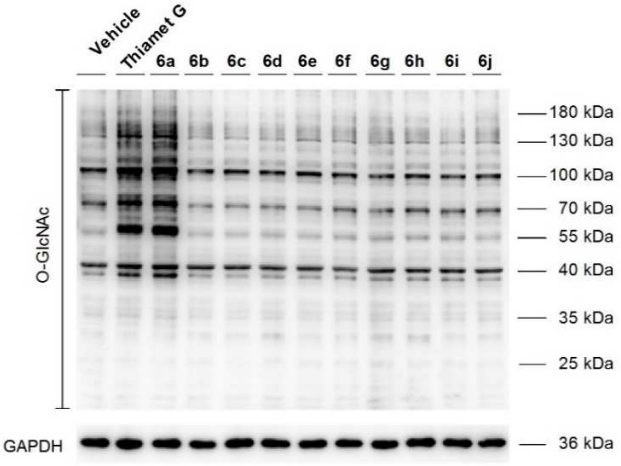

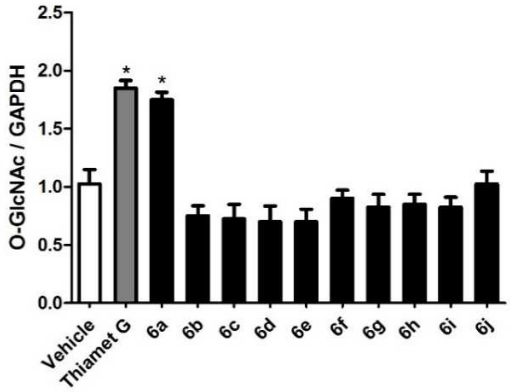

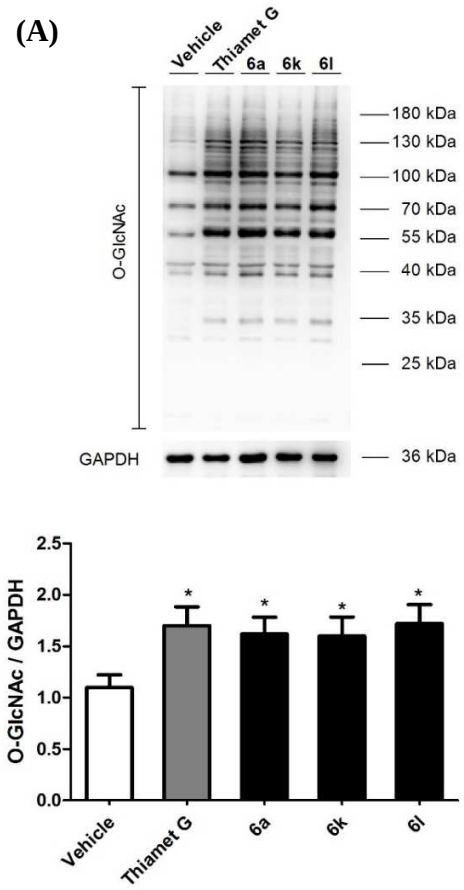

Figure 3. *O*-GlcNAc-modified proteins, determined by Western Blot analysis, in vascular smooth muscle cells (VSMCs) from Wistar rats. **(A)** Upper panel: representative Western Blot image of *O*-GlcNAc-modified proteins; Lower panel: bar graphs corresponding to the relative expression of *O*-GlcNAc-modified proteins after normalization with GAPDH. VSMCs were treated for 24 h with 1.0 µM of compounds **6a-j** and Thiamet-G (used as positive control). **(B)** Upper panel: representative Western Blot image; Lower panel: bar graphs corresponding to the relative expression of *O*-GlcNAc-modified proteins after normalization with GAPDH. VSMC were treated for 24 h with 1.0 µM of compounds **6a**, **6k**, **6l** and Thiamet-G (positive control). Results are expressed as mean ± SEM for n=5 in each experimental group. One-way ANOVA: $^{*}p < 0.05$ *vs*. vehicle.

100 μM

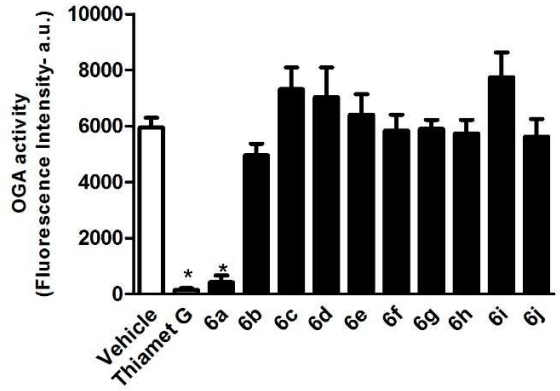

10 μM

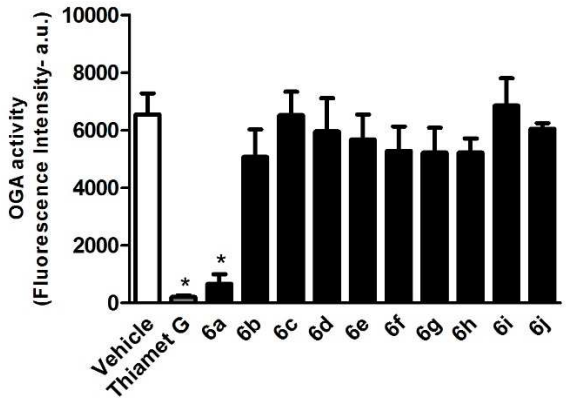

1.0 μM

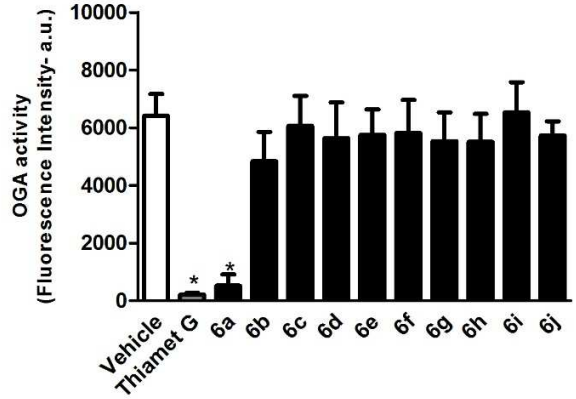

0.1 μM

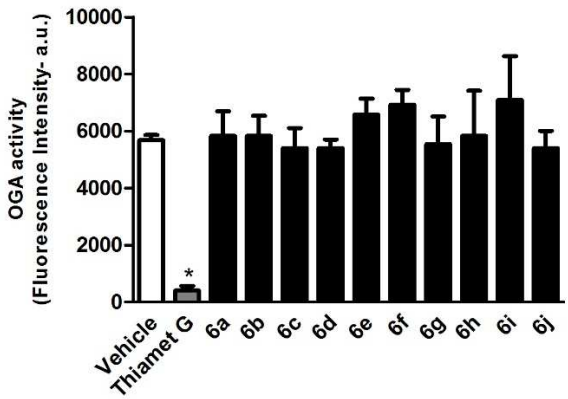

Figure 4. Inhibition of OGA activity, evaluated by a fluorimetric assay. Cultured VSMCs were treated with 4-MUNAG substrate (300 µg/ml), in the presence of vehicle or compounds **6a-j** and Thiamet-G (positive control) at various concentrations (0.1, 1.0, 10 and 100 µM). Results are expressed as mean ± SEM for n=3 in each experimental group. One-way ANOVA: $^{*}p < 0.05$ *vs.* vehicle.

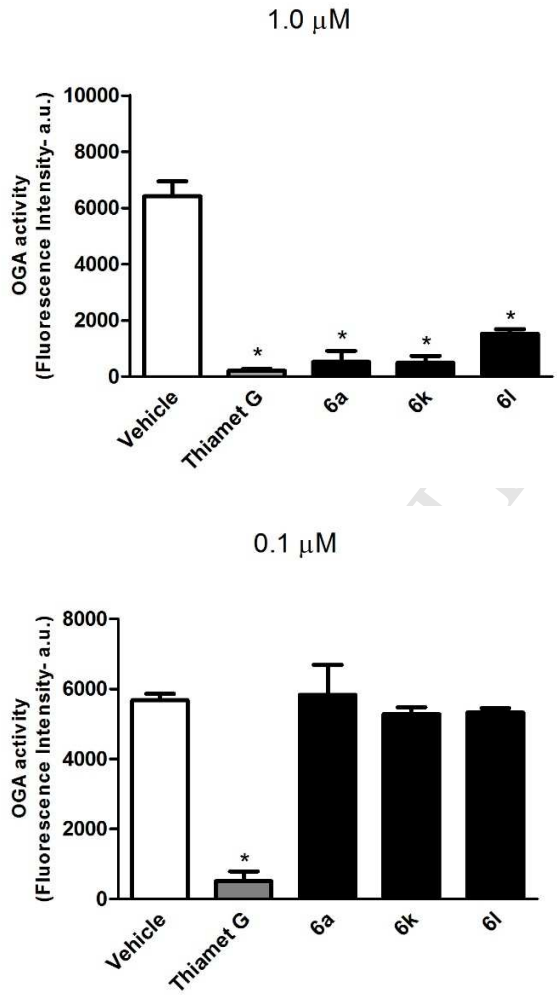

Figure 5. Inhibition of OGA activity, evaluated by a fluorimetric assay. VSMCs were treated with the 4-MUNAG substrate (300 µg/ml), in the presence of vehicle or compounds **6a, 6k, 6l**

and Thiamet-G (positive control) at the concentrations of 0.1 and 1.0 µM. Results are expressed as mean ± SEM for n=3 in each experimental group. One-way ANOVA: $^{*}p < 0.05$ *vs*. vehicle.

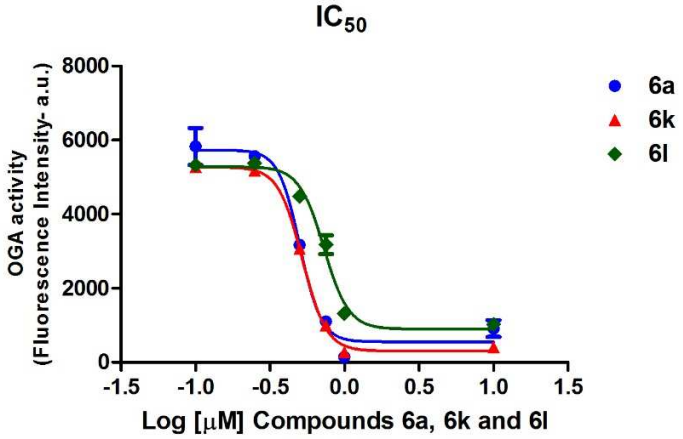

Figure 6. Concentration-response curves depicting inhibition of OGA activity. OGA activity was determined by a fluorimetric assay. VSMCs were treated with the 4-MUNAG substrate (300

µg/ml), in the presence of vehicle or compounds **6a, 6k, 6l** at the concentrations of 0.1, 0.25, 0.5, 0.75, 1.0 and 10 µM. Results are expressed as mean ± SEM for n=3 in each experimental group. Nonlinear regression: Log (inhibitor) vs. response - variable slope.

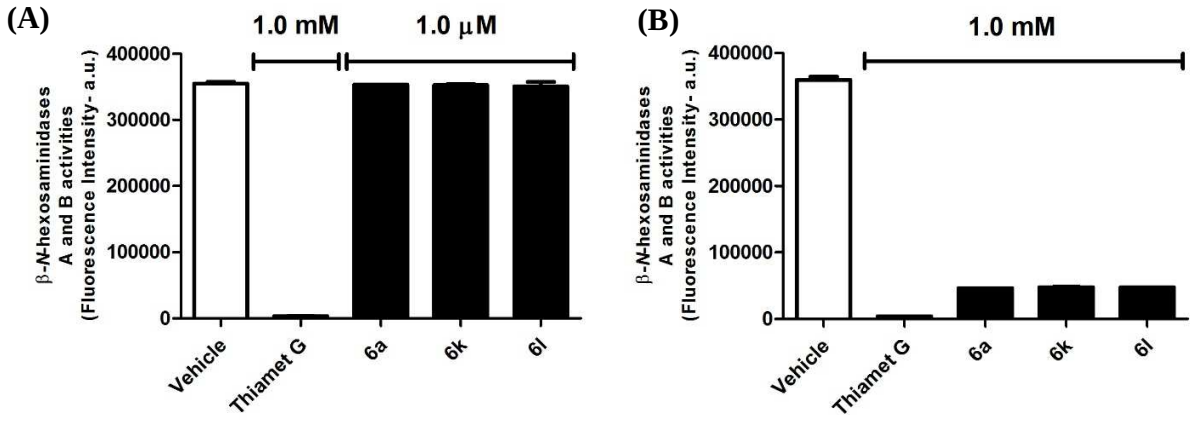

Figure 7. Inhibition of β-*N*-hexosaminidases A and B activity. HexA and B activities were determined by a fluorimetric assay. HexA and B were incubated with 4-MUNAG substrate (300

µg/ml) in the presence of vehicle or Thiamet-G (positive control) at concentration of 1.0 mM and compounds **6a, 6k and 6l** at the concentrations of 1.0 µM **(A)** or 1.0 mM **(B)** Results are expressed as mean ± SEM for n=2 in each experimental group.

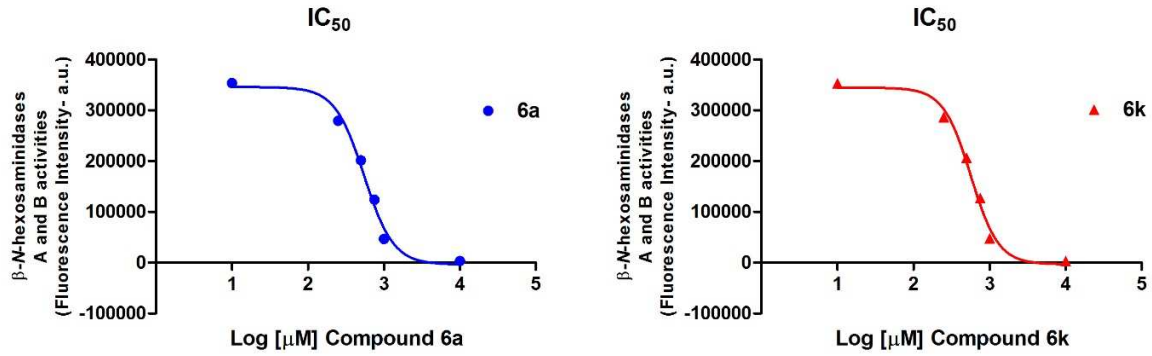

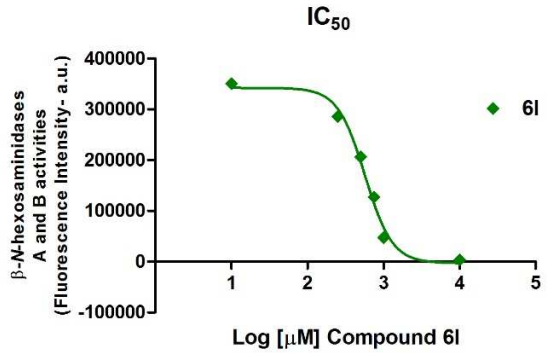

Figure 8. Concentration-response curves depicting inhibition of β-*N*-hexosaminidases A and B activity. HexA and B activities were determined by a fluorimetric assay. HexA and B were treated with the 4-MUNAG substrate (300 µg/ml), in the presence of vehicle or compounds **6a, 6k, 6l** at the concentrations of 10, 250, 500, 750, 1000 and 10000 µM. Nonlinear regression: Log (inhibitor) vs. response - variable slope.

(A)

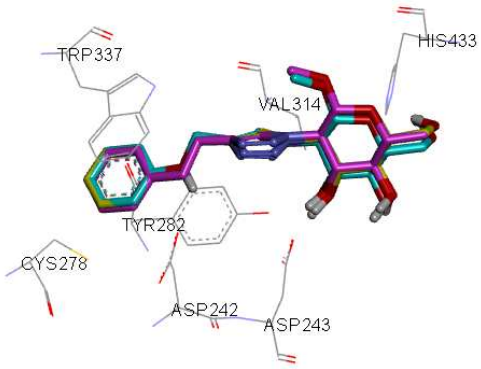

(B)

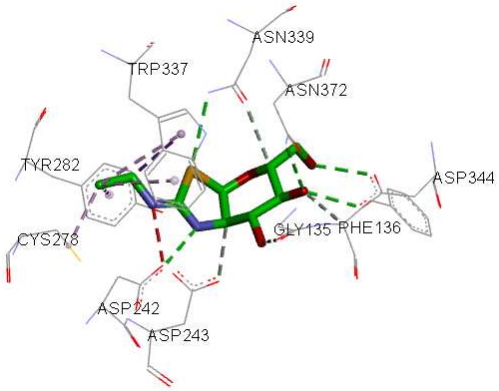

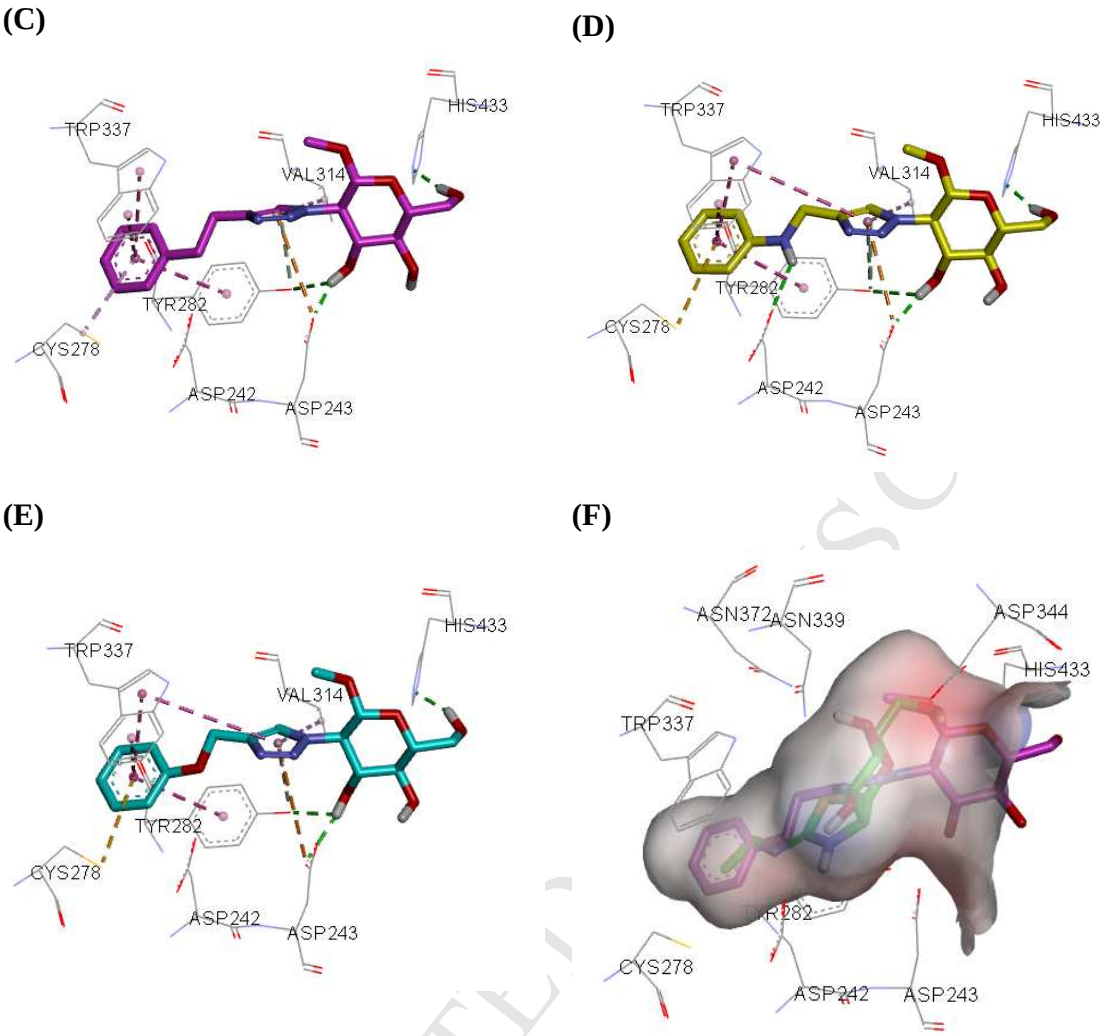

Figure 9. Diagram of Thiamet-G (crystallographic structure) and triazole compounds **6a**, **6k** and **6l** docked into BtOGA active site. **(A)**. Superposition of conformation of compounds **6a** (pink), **6k** (yellow) and **6l** (blue) obtained from docking study. **(B)**. Thiamet-G in green. **(C)**. Compound **6a** in pink. **(D)**. Compound **6k** in yellow. **(E)**. Compound **6l** in blue. **(F)**. Superposition of Thiamet-G and compounds **6a** (pink) in core catalytic domain of BtOGA. Interaction colors: in *green*, hydrogen bond interactions; in *pink*, π-π T-shape interaction; in *purple*: σ– π interaction; in orange π-anion interaction.

Scheme:

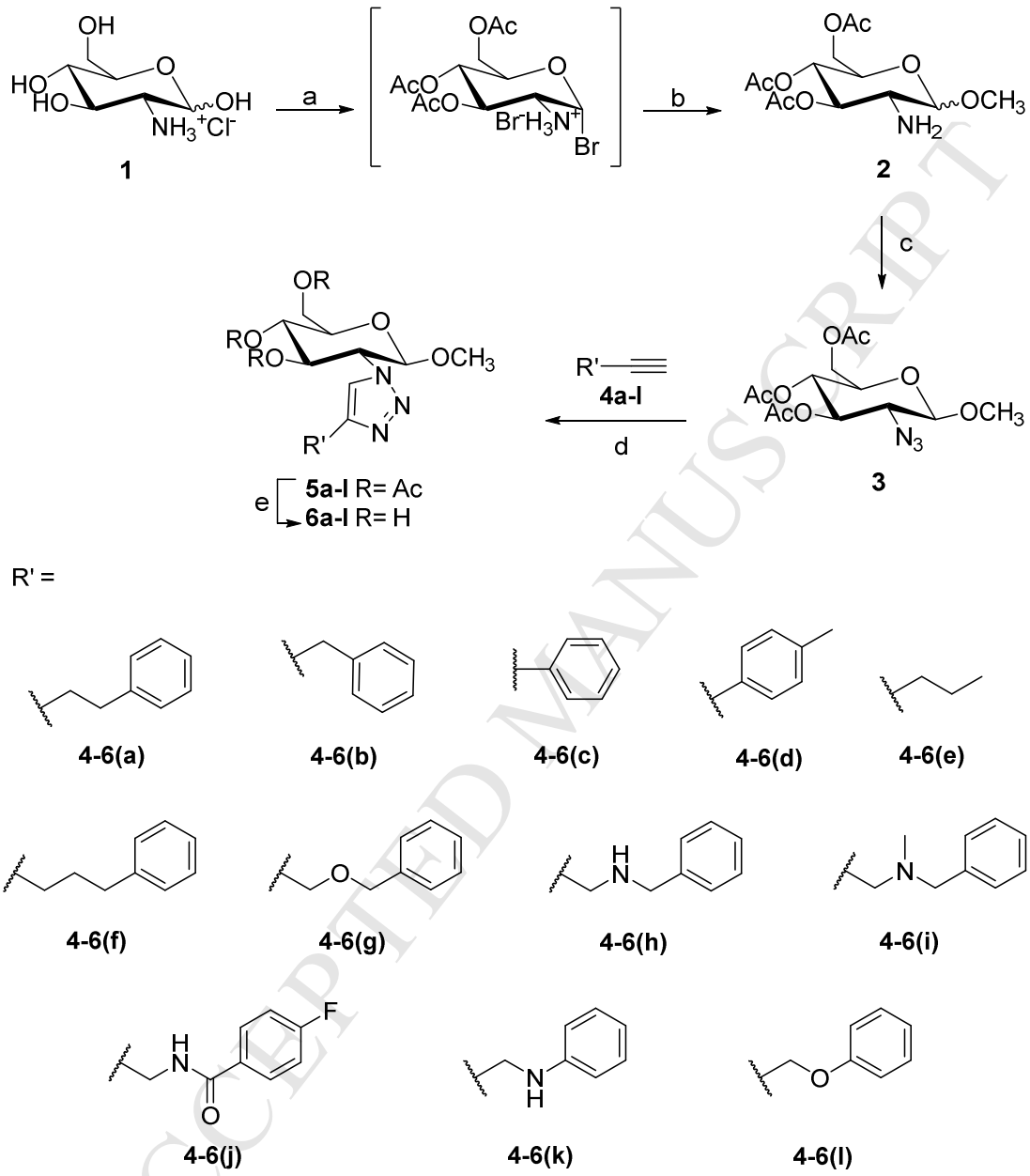

Scheme 1. Synthesis of a library of glucopyranoside triazoles **6a-l**. Reagents and conditions: (a) AcBr, r.t.; (b) MeOH, pyridine, r.t., 1 h, 61% after two steps; (c) TfN_3, triethylamine, $CuSO_4.5H_2O$, pyridine, 16 h, 37%; (d) $CuSO_4$, Na ascorbate, 43 – 93%; (e) NaOMe, MeOH, 59 – 98%.

Highlights:

- Twelve novel glucopyranoside C2-derived 1,2,3-triazoles were synthesized.
- Three derivatives were qualitatively similar to Thiamet-G in augmenting *O*-GlcNAc-modified proteins levels.
- The most potent inhibitors exhibited low micromolar activity toward OGA and high selectivity for OGA over HexA and B.
- The central chain extension bridging the C-4 position of the triazole core to the phenol ring plays a critical role for accommodation of the inhibitors in the OGA catalytic pocket.
- Glucopyranoside C2-derived 1,2,3-triazoles may be novel promising therapeutic candidates